EUROPEAN COMMISSION
Community Research

SEVENTH FRAMEWORK PROGRAMME

ARCHER

Collaborative Project (CP)

Co-funded by the European Commission under the
Euratom Research and Training Programme on Nuclear
Energy within the Seventh Framework Programme

Grant Agreement Number : 269892

Start date : 01/02/2011 Duration : 48 Months
www.archer-project.eu

Archer
Advanced Reactor
for Cogeneration of
Heat & Electricity-R&D

Test and expertise report, including results of CFD post-test calculations

Authors : PRA Franck (CEA)

ARCHER - Contract Number: 269892
Advanced High-Temperature Reactors for Cogeneration of Heat and Electricity R&D
EC Scientific Officer: Dr. Panagiotis Manolatos

Document title	Test and expertise report, including results of CFD post-test calculations
Author(s)	PRA Franck
Number of pages	53
Document type	Deliverable
Work Package	WP 43
Document number	D43.41
Issued by	CEA
Date of completion	28/01/2015
Dissemination level	Confidential, only for members of the consortium (including the Commission Services).

Summary

This document contains the experimental results obtained on the IHX mock up tested with air on CEA test rig, namely CLAIRE loop. Since delivery of the heat exchanger at CEA was delayed, final results will be provided at the end of the project. Tests are still running and an updated document will be provided. Within WP 4.3 of the ARCHER European program, a heat exchanger has been sized regarding to specification of a real helium ? helium IHX dedicated to produce high temperature vapor using a HTR reactor. This heat exchanger has been manufactured by Alfa Laval and tested on a CEA test facility at Grenoble. Tests were run on CLAIRE loop which is an air-air facility. Classical tests were run to determine the hydraulic and thermal behaviors of the bundle of the stamped plates and lead to quite good agreement with correlations obtained previously by CFD. Since these laws were used to size the mock up (and IHX), expected global performances in term of duty are reached, leading to a thermal efficiency of 90% at nominal point. At nominal working conditions, the incoloy heat exchanger was tested with a hot inlet temperature of 800°C and ~ 6.5 bars and a cold inlet temperature of 290°C and 3.5 bars. The mass flow rate was varied from 0.04 to 0.18 kg/s generating Reynolds numbers between 1000 and 5500 for the cold and hot sides respectively. Fatigue tests were run. In order to avoid any earlier damages, level of temperatures was increased progressively and specific thermal shocks were applied to the exchanger. At the present time, the hot inlet temperature is 800°C (since 20th of August 2014) and transient tests will be applied once a week with helium leak detection to check the heat exchanger behavior

Approval

Date	By
29/01/2015	Derek BUCKTHORPE
29/01/2015	Derek BUCKTHORPE
29/01/2015	Steven KNOL

Distribution list

Name	Organisation	Comments
P. Manolatos	EC DG RTD	Through the EC participant portal
All beneficiaries	ARCHER	Through the private online workspace

CONFIDENTIAL

Technical Report DTBH/RT/2015/010

«Project FP7 ARCHER - deliverable D43.41 thermal-hydraulic performances of corrugated plates HX Shock Tests analysis report – Final report »

Authors: F.Pra, S.Ben Saad

PRODEM reference	10-03377
Project title	Projet ARCHER
Period of the project	01/02/2011 – 31/01/2015
Nature of the report	☐ Progress Report ☒ Final Report ☐ Contribution to a global report ☐ Work package report (WP) ☐ Others : *specify the nature of the report* (ex : non included on the agreement, training report)
Appendices (to complete inevitably for « Restricted Distribution)	☐ YES ☒ NO If the report include appendices, specify : Appendice XX from page XXX to page XXX

	Writer (s)	Controller	Approver	Transmitter
Name	F.PRA	F.DUCROS	O.LEMAIRE	P.TOCHON
Position	Engineer	Head of laboratory	Head of Issuing Service	Head of Issuing Department
Signature				
Date	15/01/2015	22/01/2015	23/01/2015	26/01/2015

Alternative Energies and Atomic Energy Commission

T. | F.

Technological Research Division
Department : DTBH
Service : SCTR
Laboratory : LER

CONFIDENTIAL

SUIVI DES REVISIONS

Indice	Date	Motif et description de la modification
A		Document initial

CONFIDENTIAL

DISTRIBUTION LIST

Complete report signed + dispatch note signed to :

AREVA NP	D.LHACHEMI	1 ex. (email)
ALFA LAVAL	F.BAURAND	1 ex. (email)
	P.X.BUSSONNET	1 ex. (email)
	A.PECHBERTY	1 ex. (email)
	F.RONDET	1 ex. (email)
SP leader	D.BUCKTHORPE	1 ex. (email)
LITEN	Florence LAMBERT, Head of LITEN	1 ex. (email)
	Patrick DUSSOUILLEZ, LITEN Operational Director	1 ex. (email)
	Jean-Louis SIX, LITEN Marketing & Sales Director	1 ex. (email)
DEPARTEMENT:	P.TOCHON	1 ex. (email)
	Programs Correspondent	1 ex. (email)
	Assistant (Original paper storage or copy if the original is send to the customer)	1 ex (Paper)
Pilot SERVICE and LABORATORY:	O.LEMAIRE	1 ex. (email)
	F.DUCROS	1 ex. (email)
	Pilot project manager	1 ex. (email)
	Controller	1 ex. (email)
	F.PRA	1 ex. (email)

First page signed + Diffusion List + rules for document management and confidentiality + summary + dispatch note signed to :

Financial Office
Department Quality Engineer or qualite-liten@cea.fr
Only for FREE DISTRIBUTION or CONFIDENTIAL :
Heads of others departments of LITEN

CONFIDENTIAL

RULES FOR DOCUMENT MANAGEMENT AND CONFIDENTIALITY:

Based on the privacy statement shown at the top of the page, this document must be managed according to the guidelines described below.

The information contained in this document is the property of the contractors.

This document is confidential. It is communicated by XXXX (ex. « the writer of this report » if the writer is indicated in the first page) for the exclusive attention of YYY (ex. « members indicated in the distribution list » if it is included in the document) .Use or distribution to third parties unauthorized is forbidden.

FREE DISTRIBUTION: This document may be distributed to other third parties as the contractors. It must be distributed unchanged and in its entirety and include the issuer's attribution and credit. This corresponds to the type of licence defined by http://creativecommons.org/licenses/. However, recipients are requested to exercise sound judgement when redistributing the document.

CONFIDENTIAL:
This document may not be distributed to third parties other than the contractors and the direct addressees of the first transmitter.
This document may not be reproduced or transmitted to third parties without the express authorisation of the contractors.
The decision to remove the CONFIDENTIAL nature of the document rests with the issuer or comes into effect after the time specified below.

CONFIDENTIAL "PROJECT NAME":
This document may only be distributed to individuals in the project team and to individuals who require access in the course of their duties (need to know basis). Contractors are required to implement the necessary measures for complying with these distribution rules, which may be based on restricted distribution measures.
This document may not be reproduced or transmitted to third parties without the express authorisation of the contractors.
The decision to remove the CONFIDENTIAL "PROJECT NAME" nature of the document rests with the issuer or comes into effect after the time specified below.

RESTRICTED DISTRIBUTION:
This document may only be distributed to individuals in the project team and individuals who require access in the course of their duties (need to know basis).
This document could be reproduced under the responsibility of the addressee (and restricted to the strict requirements of the department) and could be transmitted under the responsibility of the holder. Pursuant to agreements between contractors (i.e, the appendix of security, necessarily signed for a project with restricted distribution), a written request to the contractors is necessary before transmission to third parties.
The management of information must comply with the requirements in Appendix 3 of the *Instruction Générale Interministérielle* (Interdepartmental General Instruction) IGI 1300 (http://www.ssi.gouv.fr/archive/fr/reglementation/igi1300.pdf), including:

1) Individuals must be informed about the rules of confidentiality.
2) The information and drafts used in drawing up the document must be labelled with the words "RESTRICTED DISTRIBUTION" and managed as such (in particular, with a recording specifying the character RD of the document).
3) The document and information used in drawing up the document must be kept under lock and key. In particular, the documents, when not in use, must be filed in a locked cabinet.
4) The document may be sent externally by letter in a double envelope (it is advisable to use a cloth lined or confidential envelope). The inner envelope must bear the words RESTRICTED DISTRIBUTION, the name of the recipient and the document reference. The outer envelope must include only the information required for the letter to be sent (the department sending the letter and the address of the recipient). It must be sent with acknowledgment of receipt. This sending should be accompanied with a dispatch note identifying the addressees.
5) The IT systems for processing, storing or transmitting the information are subject to security accreditation. When the networks or systems used are not able to guarantee confidentiality, the information is encrypted by methods approved by ANSSI (French Network and Information Security Agency). This results in the encryption of emails, computer directories, USB keys, servers, etc. using encryption approved by ANSSI. The list of equipment approved by ANSSI may be consulted on their web-site at http://www.ssi.gouv.fr/fr/produits-et-prestataires/produits-qualifies/.
6) It is the responsibility of the holder to destroy the document by shredding or incineration.
7) The decision to remove the words RESTRICTED DISTRIBUTION rests with the issuing authority alone or takes effect after the time specified below.

Pursuant to agreements between contractors, this document:

☒ is no longer confidential and does not have restricted distribution 10 years after the end of the project.

☐ is no longer confidential and does not have restricted distribution X years after the end of the project.

☐ is no longer confidential or has restricted distribution as of Click here to enter a date

☐ remains confidential or with restricted distribution for an unlimited period

CONFIDENTIAL

Table of contents

Summary

Within WP 4.3 of the ARCHER European program, a heat exchanger has been sized according to specification of a real helium – helium IHX dedicated to produce high temperature vapor using a HTR reactor.
This heat exchanger has been manufactured by Alfa Laval and tested on a CEA test facility at Grenoble. Tests were run on the CLAIRE loop which is an air-air facility.
Classical tests were run to determine the hydraulic and thermal behaviour of the bundle of the stamped plates and lead to quite good agreement with correlations obtained previously by CFD. Since these laws were used to size the mock up (and IHX), the expected global performance in term of duty were reached, leading to a nominal thermal efficiency of 90%.
At nominal working conditions, the incoloy heat exchanger was tested with a hot inlet temperature of 800°C and ~ 6.5 bars and a cold inlet temperature of 290°C and 3.5 bars.
The mass flow rate was varied from 0.04 to 0.18 kg/s generating Reynolds numbers between 1000 and 5500 for the cold and hot sides respectively.
Fatigue tests were carried out and in order to avoid any earlier damage, the level of temperature was increased progressively and specific thermal shocks were applied to the exchanger.

A progress report was issued at the end of September. The present report is the final version which includes further tests performed up to the end of the ARCHER project.
At the present time, tests at 800°C are still going on.

Key words

High-temperature, Compact heat exchangers, IHX, thermal performances, hydraulic performances, thermal shocks, helium tests, Claire loop.

EUROPEAN COMMISSION

Community Research

ARCHER

Collaborative Project

Co-funded by the European Commission under the
Euratom Research and Training Programme on Nuclear Energy
within the Seventh Framework Programme

Grant Agreement Number: 269892

Start date: 01/02/2011 Duration: 48 Months

www.archer-project.eu

Test and expertise report

Franck PRA (CEA)

ARCHER project – Contract Number: 269892

Advanced High-Temperature Reactors for Cogeneration of Heat and Electricity R&D

EC Scientific Officer: Dr. Panagiotis Manolatos

Document title	Test and expertise report
Author(s)	Franck PRA (CEA)
Number of pages	**51**
Document type	Deliverable
Work Package	WP4
Document number	D43.41 – revision 0
Issued by	CEA
Date of completion	15/01/2015
Dissemination level	Restricted to the partners of the ARCHER project/Public

CONFIDENTIAL

Summary

This document contains the experimental results obtained on the IHX mock up tested with air on CEA test rig, namely the CLAIRE loop. Since delivery of the heat exchanger at CEA was delayed, a preliminary version of the report was issued in September 2014 and the present report is an updated version containing results up to the end of the ARCHER project.

At present time, tests of the heat exchanger are still going on.

Approval

Rev.	Short description	First author	WP Leader	SP leader	Coordinator
0	Final issue	PRA (CEA) 15/01/2015	D.LHACHEMI (AREVA)	D.BUCKTHORPE	S.KNOL(NRG) ../../..

Distribution list

Name	Organisation	Comments
P. Manolatos	EC DG RTD	
All technical participants	ARCHER	
Steering Committee members	ARCHER	

Introduction

Workpackage 4.3 of the European Research program ARCHER covers the demonstration of the feasability of an IHX module including :

- the design;
- manufacture of a mock-up made from Alloy 800H;
- tests in the Claire loop at operating conditions (750°C-800°C) to assess the compact IHX, namely PSHE, lifetime.

CFD and FEM calculations are performed on an IHX with real working conditions and on a mock up with air Claire loop working conditions. CFD calculations aim to predict the thermal and hydraulic performance of the devices and to provide temperature fields for FEM calculations. These calculations are carried out under nominal steady conditions and under transient conditions. CEA performs CFD calculations using the FLUENT software and temperature fields are respectivily provided to NRG and Alfa Laval to carry out FEM calculations for the air mock-up and the real IHX.
In the first part of this report, the main objectives of the study and information on the heat exchanger and Claire test rig are given, also the hydraulic and thermal performance under steady state are analysed and compared with predictions. In the second part, specific tests related to the thermomechanical characteristics are presented.

1. OBJECTIVES OF THE STUDY

Within the WP 4.3, a complete IHX has been sized using inlet data from AREVA. The specifications are dedicated to a 600 MWth nuclear gas reactor to produce heat at high temperature. Table 1 provides the nominal working conditions of the IHX in steady state.

	Primary hot fluid		Secondary cold fluid
Fluid	helium		helium
Mass flow rate (kg/s)	251		251
Inlet Temperature (°C)	750		240
Expected Outlet temperature (°C)	290		700
Expected thermal efficiency (%)		90	
Expected Thermal Duty (MW)		600	
Inlet pressure (bar)	55.1		50.2
Allowed ΔP (% Pin)	2		2

Table1 : Steady state working conditions for the IHX

Considering these data, the IHX was sized to reach the required thermal and hydraulic performance.

With regard to the main characteristics of air Claire test rig, a specific mock-up was sized and manufactured by Alfa Laval.

1.1 Main characteristics of the IHX and the mock up

- Plate sizes are determined by previous studies and technological aspects: Width, length and thickness of the plates.
- The hydraulic diameter is the same for both sides and is chosen to have a compact technology with respect to the allowed pressure drops.
- The height of the stack for the whole IHX (number of plates per module) is determined by FEM consideration.
- The active area is made of corrugated plates
- Plate thickness = 1.5 mm
- Depth of corrugation = 1.5 mm
- Thermal and hydraulic laws of the chosen geometry are quite well known (CFD – preliminary test)
- Plates are stacked and contact points ensure rigidity of the HX
- Along the edges and around the collectors, laser welding is used.

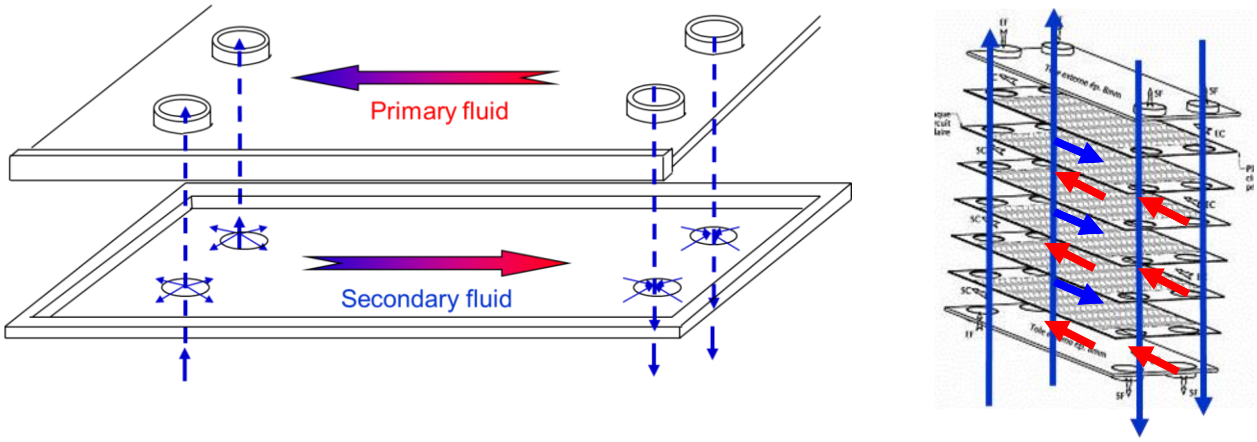

Figure 1 : Sketch of flow distribution in the heat exchanger

CONFIDENTIAL

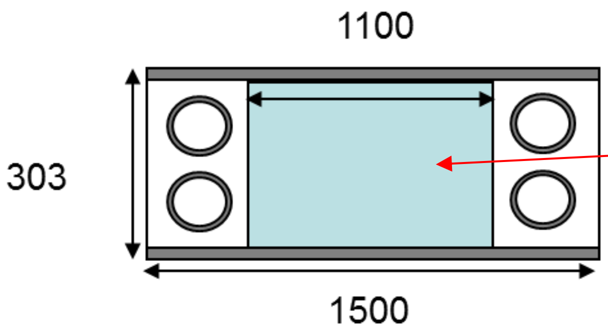

Main geometrical characteristics

Stamped plate in the thermal active area

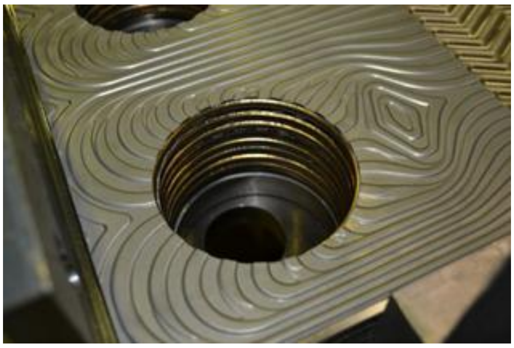

Distributing area for cold fluid : cold fluid flows in the holes to go inside (or outside) the channels

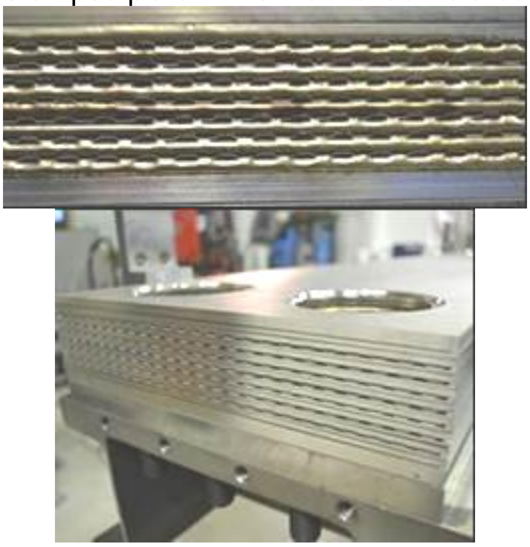

Hot fluid flows in straight direction through the passages

Figure 2 : Details of the plates

	Primary fluid		Secondary fluid	Primary fluid		Secondary fluid
	He		**He**	**Air**		**Air**
Mass flowrate (kg/s)	251		251	0,18		0,18
Inlet T (°C)	750		240	800		290
Expected Outlet T (°C)	290		700	340		750
Expected Thermal Duty (MW)		600			91 kW	
Expected Thermal efficiency (%)		**90**			**90**	
Pin (bar)	55		50	6		6
Allowed DP (% Pnom)	2		2			
Plate						
Lenght (m)		1,5			1,5	
Active lenght (m)		1,100			1,100	
Height of the module (m)		0,495			0,024	
Number of modules		128			1	
Number of plates / module		165			16	
Total volume (m^3)		20,90			0,016	

Table 2: Comparison between He IHX and Air mock up

1.2 Main characteristics of CLAIRE test rig

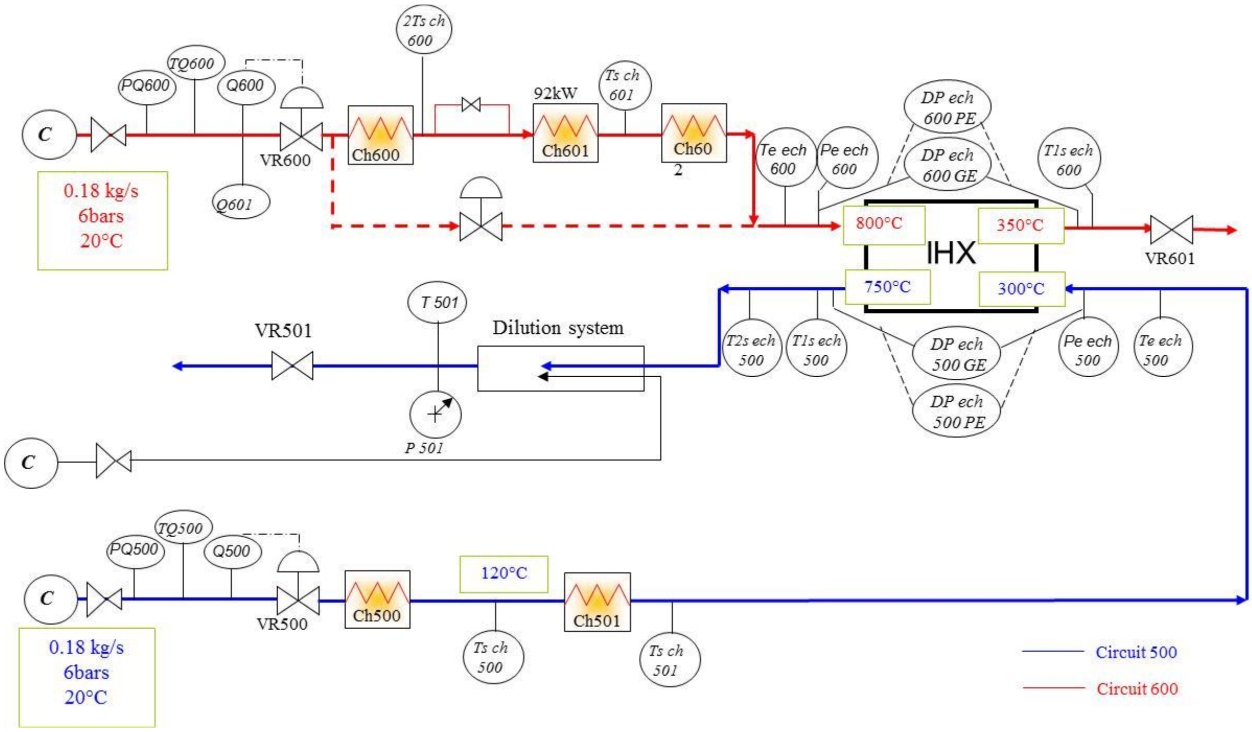

Figure 3 : Sketch of CLAIRE loop

The CLAIRE test rig is an open air loop. Air flow is generated by a compressor which fills a tank to limit the unsteadiness of the flow. From the tank, two independent circuits are connected to the mock up. The first one, C600, stands for the hot fluid circuit and the second one, C500, for the cold one. In each circuit, electrical heaters are used to heat the air. In the hot circuit, three heaters are used whereas in the cold one, two heaters are used.

On the hot side C600, it is possible to partially bypass the three heaters, so that by regulation we may generate thermal shock by injecting cold air into the hot air at the outlet of the third heater.

The mass flow rate is limited to 0.18 kg/s. These data was considered to define the number of plates in the mock up since we wanted it to follow the real helium IHX regimes in term of Reynolds numbers.

The working pressure is also an important limitation:

For this application, it has been decided to choose an inclined technology to withstand the thermo mechanical stresses. So, it is necessary to have an “elastic structure”. As said previously, the plates are stacked together without internal welding; the plates are welded only along the edges. Plates are able to stand pressure differences of few bars but they can’t stand a dozen bars without external pressure. This is the reason why the bundle of plates is inserted within a vessel. The vessel is under pressure and the pressure level is generated by the hot inlet fluid.

Specific care has to be paid in the design as explained below.

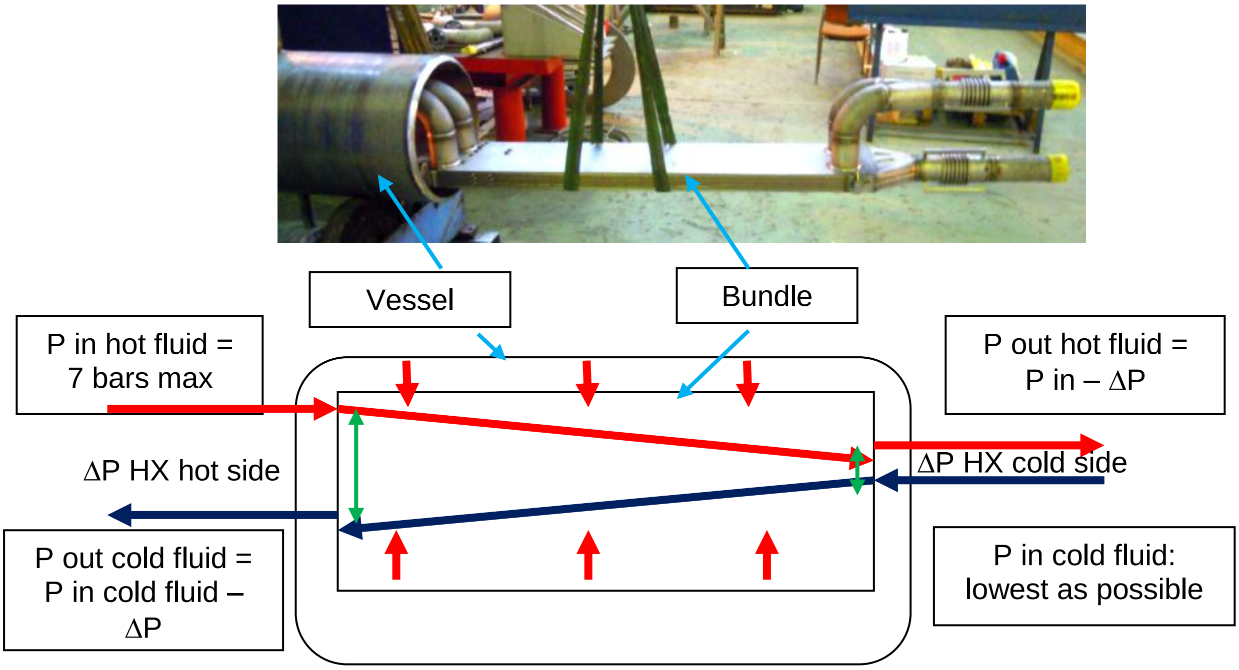

- ΔP HX hot side = P in hot fluid – P out cold fluid always >0

The pressure in hot fluid is limited by the allowed working pressure in electrical heaters (i.e. 7 bars) In an ideal case, we would like to have a difference of pressure of around 5 bars at the hot part of the heat exchanger to generate damage.

- ΔP HX cold side = P out hot fluid – P in cold fluid

The pressure in the cold fluid has to be set at the lowest value to decrease the P out cold fluid. For mechanical reasons, ΔP HX cold side has to have the same sign as the ΔP HX hot side. To protect the bundle of plates, a safety device is used within the controlling device to check that ΔP HX cold side is always higher than 0.5 bar.

So considering pressure limitation of the heaters, pressure safety devices, pressure drops inside the bundle and in regulation valves, compromises have to be found in term of working pressure for the high mass flow rates tests and high temperatures (both generating high pressure drop).

CONFIDENTIAL

1.3 Views of the whole heat exchanger

Figure 4 : Pictures of the vessel

The vessel is under pressure and as said previously it is connected to high pressure circuit (hot side). The vessel is filled with mineral products to limit heat losses and is insulated on the outside.

Thermocouples are located on the outer plate.

Figure 5 : Pictures of the vessel and thermocouples

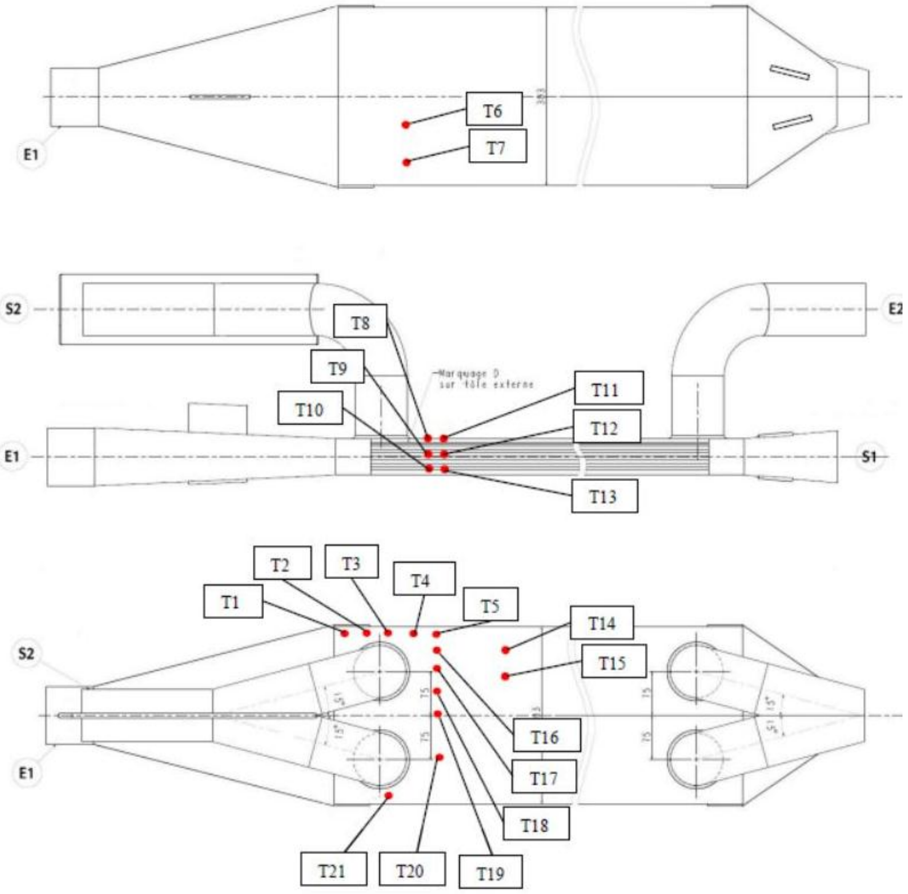

Figure 6 : Location of 21 thermocouples on the outer plate

2. TESTS AND PLANNING

To estimate the performance of the heat exchanger, certain tests are required:

Thermal and hydraulic behaviour under steady state:

- Hydraulic tests → determination of friction law with dimensionless numbers
- Thermal tests → determination of thermal law with dimensionless numbers

Thermo mechanical behaviour:

It is quite difficult to make an extrapolation between a mock up and a module. It was decided to have the same main plate dimension (length, width) but it was impossible to have the same number of plates.

From past experience, thermo-mechanical calculations showed the most damaging factor seems to be creep rather than fatigue linked to thermal shocks. Both phenomena are experimentally tested on the mock up by generating thermal shocks and by increasing the working temperatures by 50°C compared to IHX ones. This increase of temperature should accelerate damage linked to creep.

The following test planning was initially proposed and experimentally applied:

1 Hydraulic tests: at ambient temperature, pressure drops are measured between the inlet and outlet on both circuits. It is a usual practice to run these tests at ambient temperature and since the extracted friction laws are based upon dimensionless parameters, it's possible to use them later to predict pressure drop whatever the temperature and pressure. Nevertheless, we have to ensure that the range of validity of the laws in terms of Reynolds number is maintained.
The tests were run at different pressures to check the potential decrease or increase of the flow section under pressure load.

2 Thermal tests:
The working temperatures were progressively increased and thermal laws extracted to qualify the heat exchange ability of this technology. As previously, the level of temperature shouldn't influence the results but they may be affected by thermal losses, the flow distribution (linked to pressure drops), longitudinal thermal conduction, etc…

3 Thermo mechanical tests:
The increase in temperature was made progressively. Once the thermal and hydraulic tests were finished, thermal shocks were applied in the following way:

Hot inlet temperature	Hot inlet temperature variation	Time duration of the campaign	Number of shocks
650°C	100°C	1 week	As many as possible
	150°C	1 week	?
	200°C	1 week	?
Helium leak detection			
700°C	200°C	1 week	?
Helium leak detection			
750°C	200°C	1 month	~ 1 / week
Helium leak detection			
800°C	200°C	1 month	~ 1 / week
Helium leak detection			

Cold inlet temperature is kept constant = 290°C

Table 3: Agenda of tests

A specific procedure was used to detect eventual leaks in the HX, either within the bundle (directly between hot and cold sides of the bundle) or through the outside wall of the bundle.
This method consists of injecting helium either into the hot circuit or the shell. A helium sensor is used in the secondary circuit to detect a leak or not.

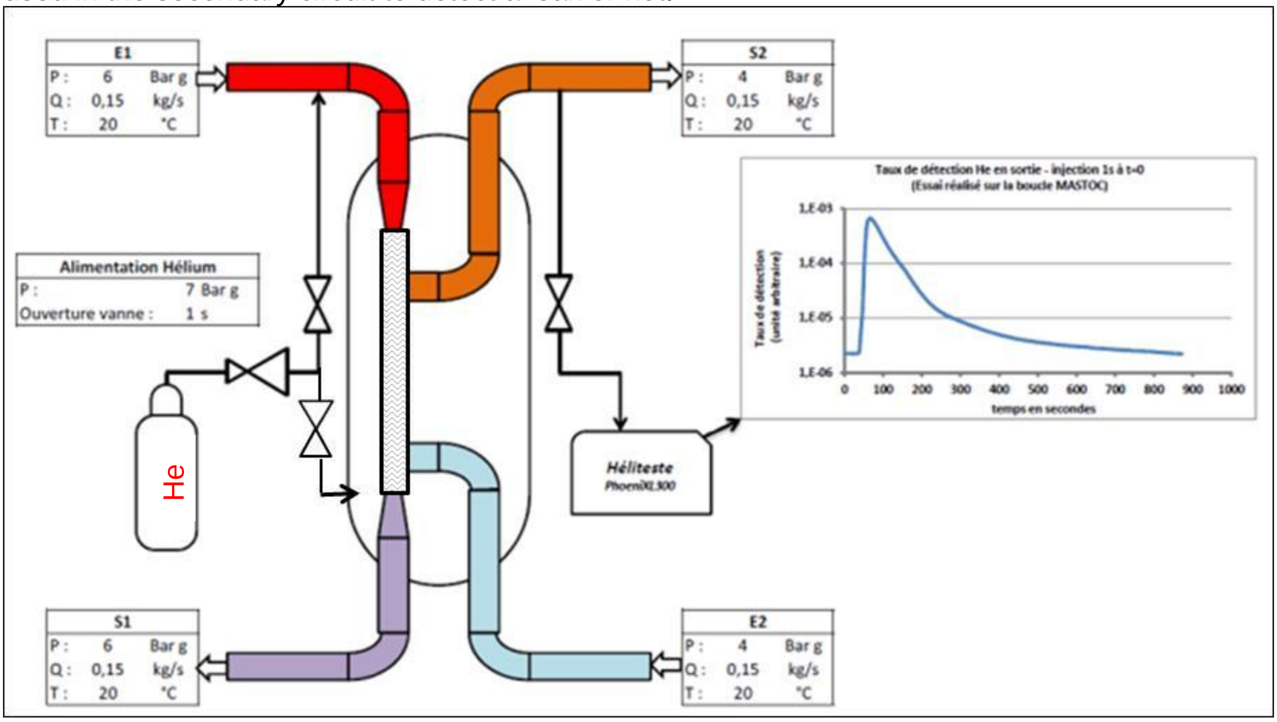

Figure 7 : Leak detection

A specific procedure was applied to periodically check the state of the HX. By always injecting the same amount of helium, we are able to look if the outlet signal evolves or not.

During the manufacturing of the HX, a very small leak was detected by Alfa Laval. This leak has no effect in terms of the global performance for the HX and it was decided with partners to not repair it since it could have been more damaging. This default is in fact an opportunity for us to calibrate the helium leak detection system (amount of helium and duration of helium injection). Since we have a plot of the response time, it is used as a reference. The superposition of the different measurements allowed us to see if there is an evolution or not of the leak. The method must be considered as a quantitative and not qualitative solution as we can't estimate the size of a leak.

3. HYDRAULIC PERFORMANCES OF THE HEAT EXCHANGER

The friction characteristics of the heat exchanger are obtained from the differential pressure measurements across each fluid sides (hot and cold sides).
For both air-sides, all physical properties such as a density, viscosity were calculated based on the inlet/outlet/average temperature and pressure of each side of the heat exchanger. Friction factor (*f*) is calculated from:

$$f = \frac{\Delta P \, D_h}{2L \, \rho V^2} \qquad (1)$$

With:
ρ : Density (kg/m^3)
V : velocity (m/s)
Dh : Hydraulic diameter (m)
L : length of the plate (m)

The measured pressure drop (ΔP) is a global measurement between inlet and outlet. The main contribution of the whole pressure drop should be generated by the active length of the plate. Distributing areas, pipes, inlet and outlet effects should be around 10% of the whole pressure drop.

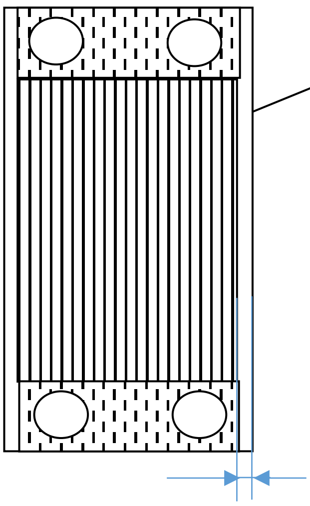

Hydraulic diameter (mm)	2.54
Depth of stamping (mm)	1.5
Length (mm)	1500
Active length (mm) (stamped length)	1100
Active width (mm) (stamped width)	288
Gap between corrugated plate/edge (mm)	4.5

4.5 mm

Figure 8 : Main geometrical data of the corrugated plate

The experimental results are compared with correlations obtained from the CFD simulations on such corrugations.
The reference friction correlation is the following one:

$$f = 1.44\, Re_{Dh}^{-0.32} \qquad (2)$$

Where Re_{Dh} is Reynolds number defined as:

$$Re_{Dh} = M\, Dh/\mu\, Acc \quad (3)$$

M : mass flow rate (kg/s)
µ : dynamic viscosity (Pa.s)
Acc : free flow area (m^2)

Different approaches were used to extract the friction law from the measurements.

1 Using global measurements

From global pressure measurements friction coefficients are directly calculated using (1) i.e. without any correction.

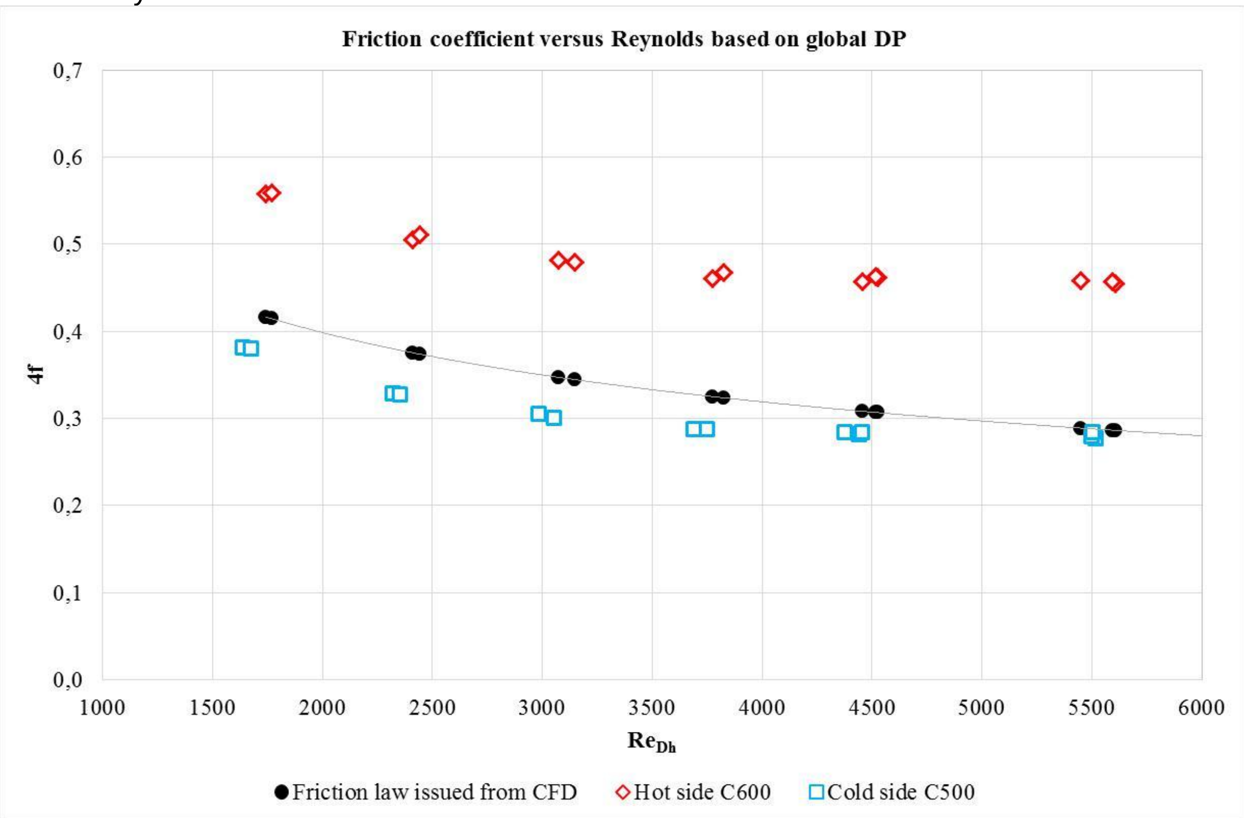

Figure 9 : Friction law using global ΔP

Figure 9 shows clearly that the friction coefficients estimated on the hot side are much higher than those on the cold side if global ΔP measurements are used without corrections on measurements. Since the plates have the same pattern on both sides, we should obtain similar hydraulic behaviour when looking at the active area behaviour.

Nevertheless, at first sight the friction law obtained by CFD simulation is bordered by experimental measurements so the analysis has to be refined.

2 Taking into account distributing areas

Before reaching the active part of the plates, the fluid distribution is different from one side to the other as shown below.

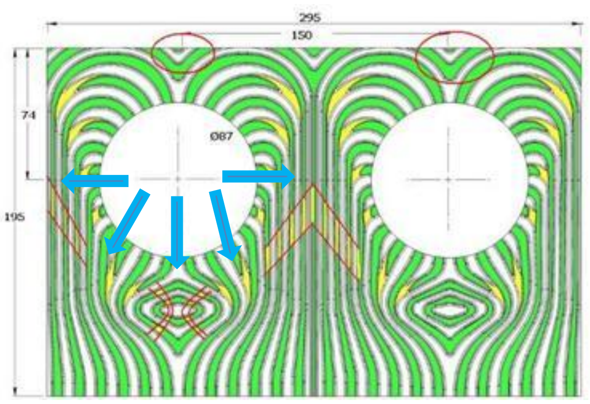

On cold side, air coming out (at inlet) from holes tends to flow directly to the active part of the plate.

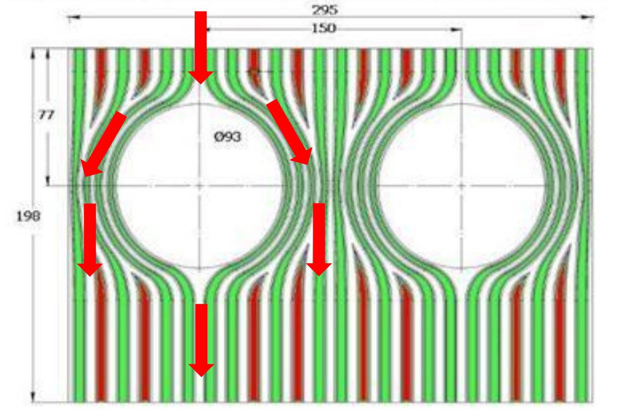

On hot side, air has to flow around the holes to reach the active part of the plate :

- Change of free flow area
- Longer length of flow

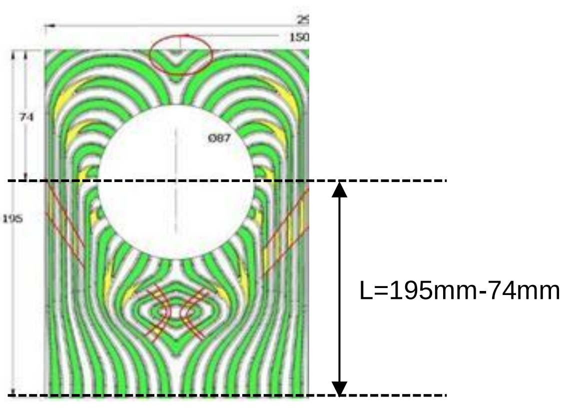

Cold side distribution

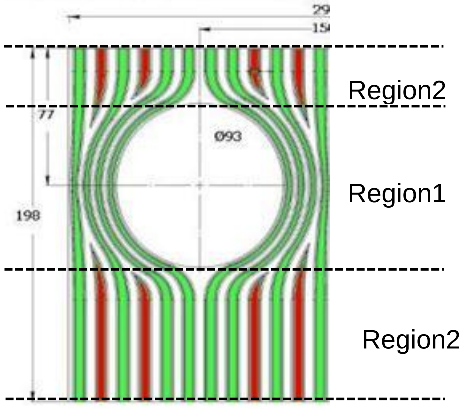

Hot side distribution

Figure 10 : Detail and comparison of fluid distribution area

The global pressure drop is corrected for both sides considering:

- These different parts within the distributing areas
- The thickness of the inserts used in these areas to deflect the fluid flow

CONFIDENTIAL

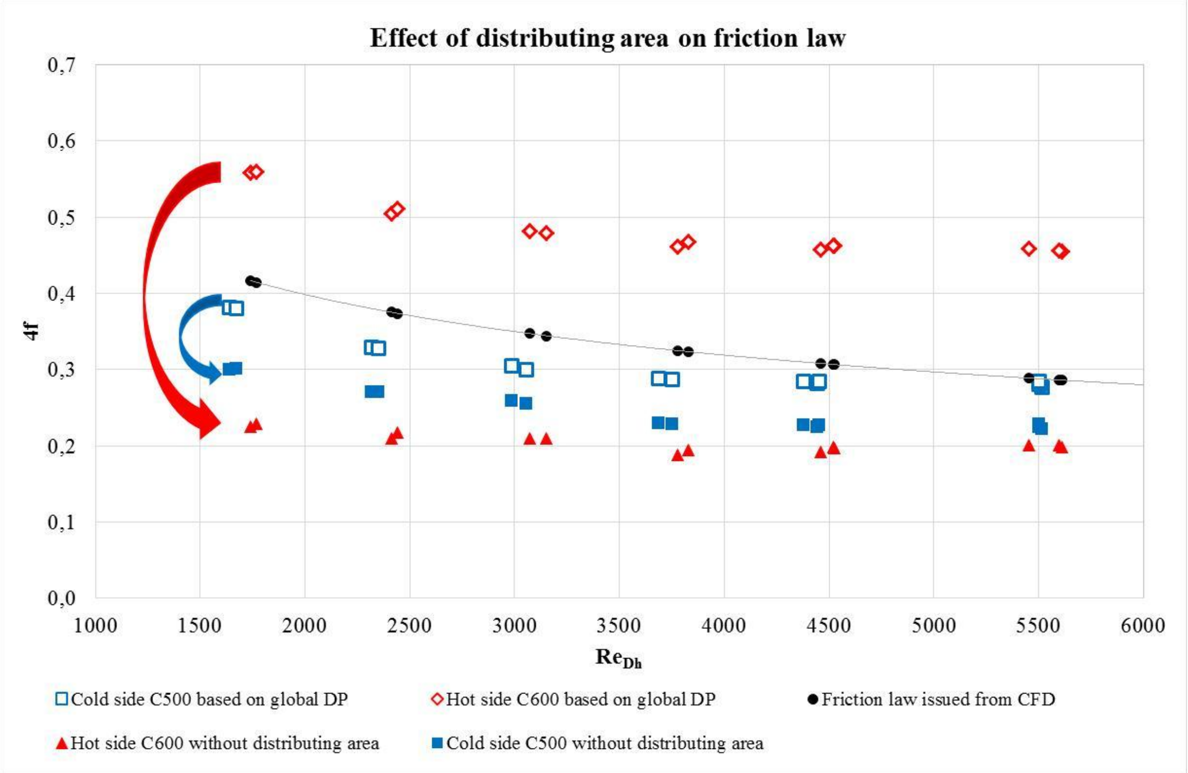

Figure 11 : Friction laws corrected by distributing areas effects

As shown in figure 11, friction coefficients are strongly affected by the correction made on the pressure drops due to inlet and outlet distributing areas. Initial results are included on the graph so that we can see the different effects on both sides. Since friction coefficients calculated in the active part have decreased for both, the experimental data are now lower than the predicted value issued from CFD. The correction means that the experimental data was closer than determined initially.

3 Further refinements

Due to manufacturing technology, plates can't be stamped along the whole width of the plate. In fact, there is a gap along the longitudinal edges acting as a flow bypass.

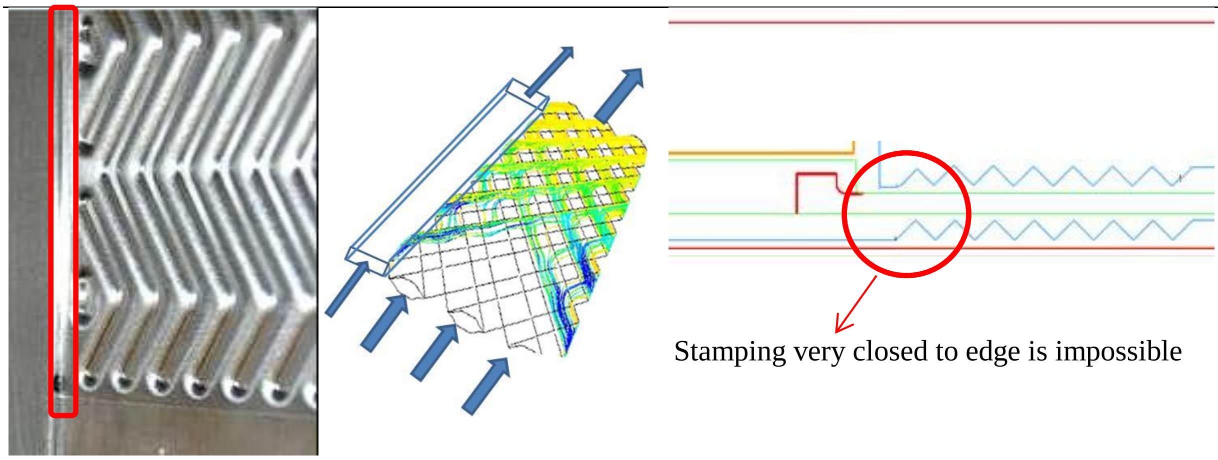

Figure 12 : Bypass along longitudinal edges

Considering a stamped area of 288 mm width generating a given pressure drop and having two bypasses along the edges of few mm width but lower friction coefficient, it is possible to estimate the percentage of flow in these gaps.
Since we aim to check the hydraulic performances of the stamped area and to compare friction coefficients with CFD results, it is necessary to correct the mass flow in the stamped plate.

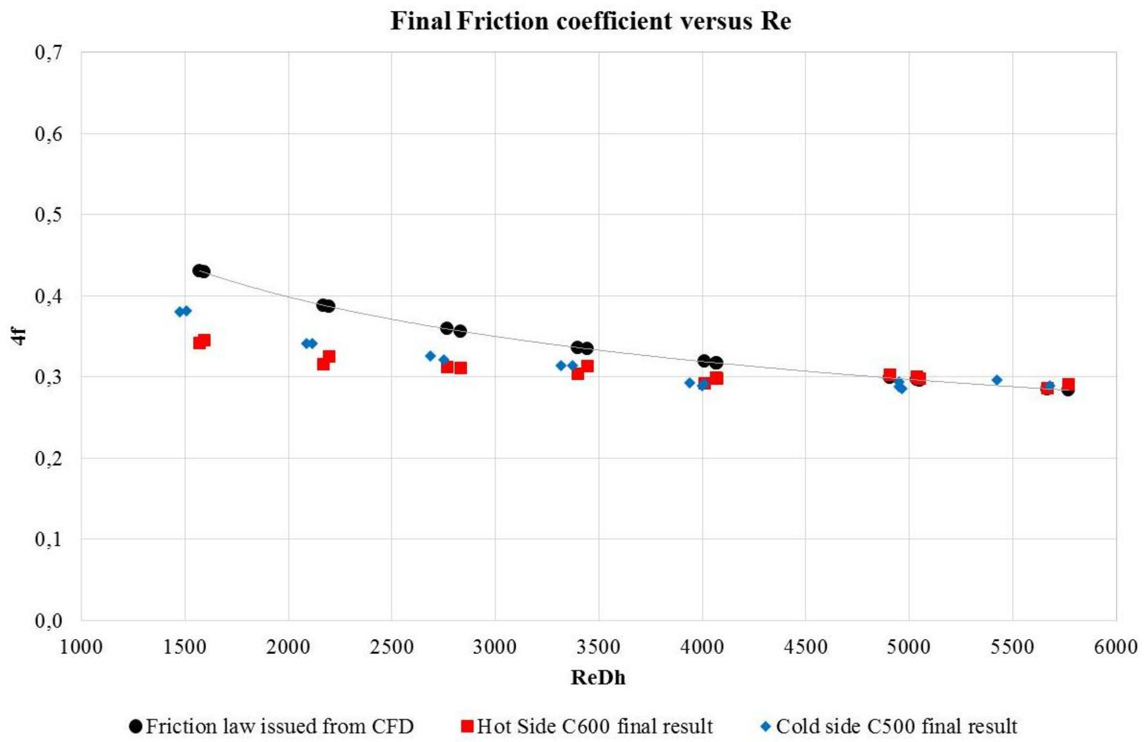

Figure 13 : Final friction coefficients

Over the range of Reynolds number between 1500 and 6000, corrected friction coefficients obtained on the cold and hot side of the heat exchanger are very close (as expected since the plate geometry is identical). When comparing with the CFD results, we may conclude that the results are satisfactory, especially at high Reynolds numbers.

4. THERMAL PERFORMANCE OF THE HEAT EXCHANGER

In the same way as the hydraulic performance, we can determine the thermal performance of the plates based on temperature measurements at the inlet and outlet of the heat exchanger.
The approach involves determining the Nusselt number versus the Reynolds number. This approach still uses a dimensionless number so that it may be used whatever the temperature, pressure and physical properties. The variation in Nusselt number is also compared with the results obtained using CFD.
For hot and cold sides, the physical properties such as density, conductivity, viscosity, Prandtl number and specific heat were calculated based on the inlet/outlet/average temperature and pressure of each side of the heat exchanger.

Procedure to analyze the results:
As previously, two methods were used to analyze the thermal performance.

1st method with global measurements:
From temperature measurements and mass flow rates, the thermal power is calculated for each side.

$$Q_{h,c} = (Mcp)_{h,c}(Tin - Tout)_{h,c} \qquad (4)$$

For further calculations, average thermal power calculated on hot and cold sides will be used, namely Q.

In order to evaluate the thermal performance of the heat exchanger, it is necessary to calculate the mean temperature difference between the hot and cold fluids. Logarithmic mean temperature difference (LMTD) in the plate heat exchanger is defined as:

$$LMTD = \frac{(T_{h,in} - T_{c,out}) - (T_{h,out} - T_{c,in})}{ln\left[(T_{h,in} - T_{c,out})/(T_{h,out} - T_{c,in})\right]} \qquad (5)$$

The overall heat transfer coefficient (U) is the ratio between the average exchanged thermal power (Q) and the heat transfer area (A) and the LMTD:

$$U = \frac{Q}{A.LMTD} \qquad (6)$$

$$A = (2N - 1) * L * \mathrm{W} \qquad (7)$$

With N: number of fluid channels per fluid (i.e: 8 for cold fluid and 7+2*1/2 for hot fluid)

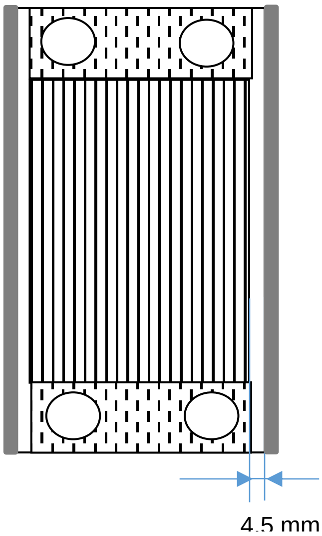

Parameters	Values	unit
Hydraulic diameter	2.54	mm
Total Length of the plate	1500	mm
Total width of the plate	303	mm
Active Width (Wst) (stamped length)	288	mm
Width between longitudinal edges (W)	297	mm
Active Length (L) (stamped length)	1100	mm
Gap between corrugated plate/calendar	4.5	mm

Figure 14 : Recall of geometrical parameters of the corrugated plate

First approximation: since tests are realized at same *M*Cp* between both fluids, the local heat exchange coefficient is extracted as follows:

$$h_{h,c} = \frac{2}{\left[\frac{1}{U} - \frac{e}{\lambda}\right]} \qquad (8)$$

e : thickness of the plate (m)
λ : thermal conductivity of the incoloy (W/m/K)

$$Nu_{\ h,c} = \frac{h_{h,c\ Dh}}{\lambda_{h,c}} \qquad (9)$$

$\lambda_{h,c}$: thermal conductivity of fluids (W/m/K)

Inlet temperatures and flow rates were increased progressively and the corresponding thermal results plotted on figure 15. Using dimensionless numbers allows comparisons to be made between tests whatever the level of temperature.
The experimental results are compared with the correlations obtained from the CFD simulations.
The reference Nusselt correlation is as follows:

$$Nu = 0.41 {Re_{Dh}}^{0.538} Pr^{1/3} \qquad (10)$$

With:
Pr : Prandtl number

$$Pr = \left(\frac{\mu\ Cp}{\lambda}\right)_{fluid} \qquad (11)$$

Cp : specific heat (J/kg/K)

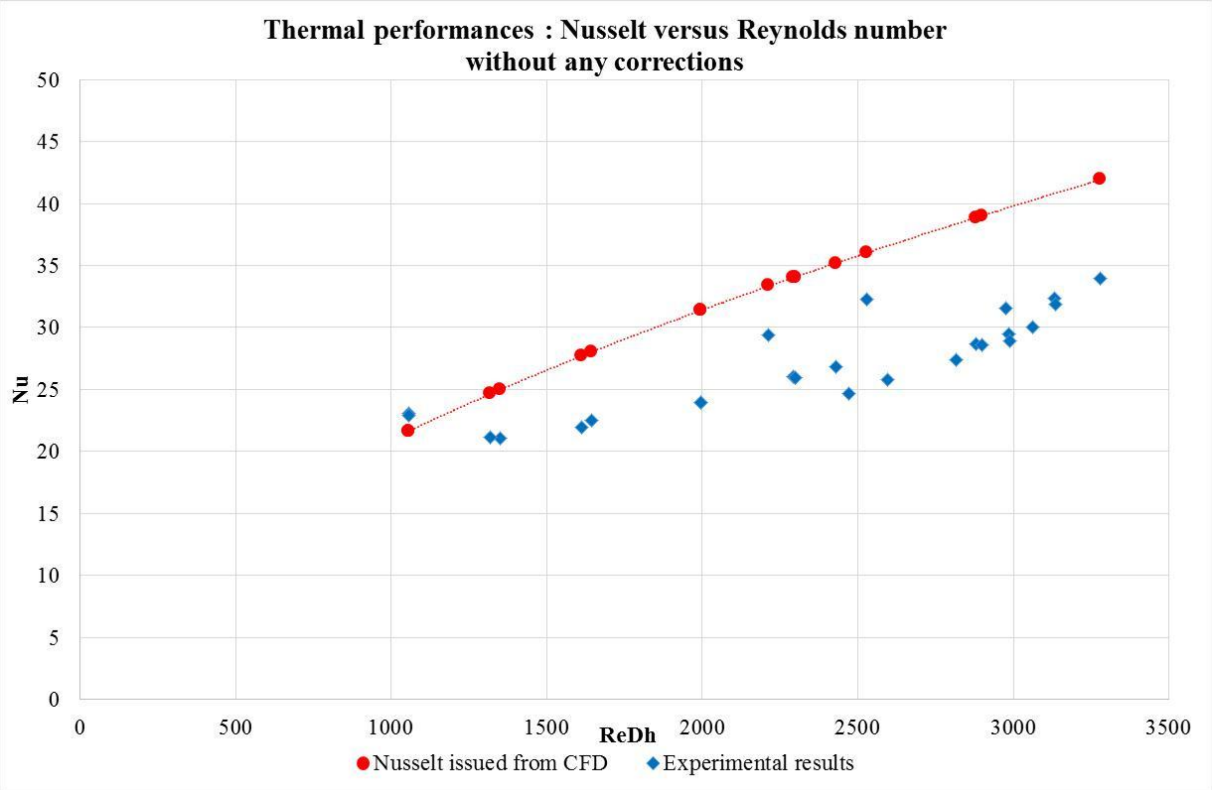

Figure 15 : Thermal performances without any corrections

Looking at the thermal performance results of figure 15, we can conclude that the thermal performance of the global heat exchanger is lower than the predicted one issued from CFD. Nevertheless the global performance of the heat exchanger respects the specifications since the expected thermal efficiency is reached.

The thermal efficiency of the heat exchanger is defined as the ratio between real thermal duty and maximum thermal power which can be exchanged.

$$\varepsilon = \frac{Q}{(mCp)_{min}(Tin_h - Tin_c)}$$

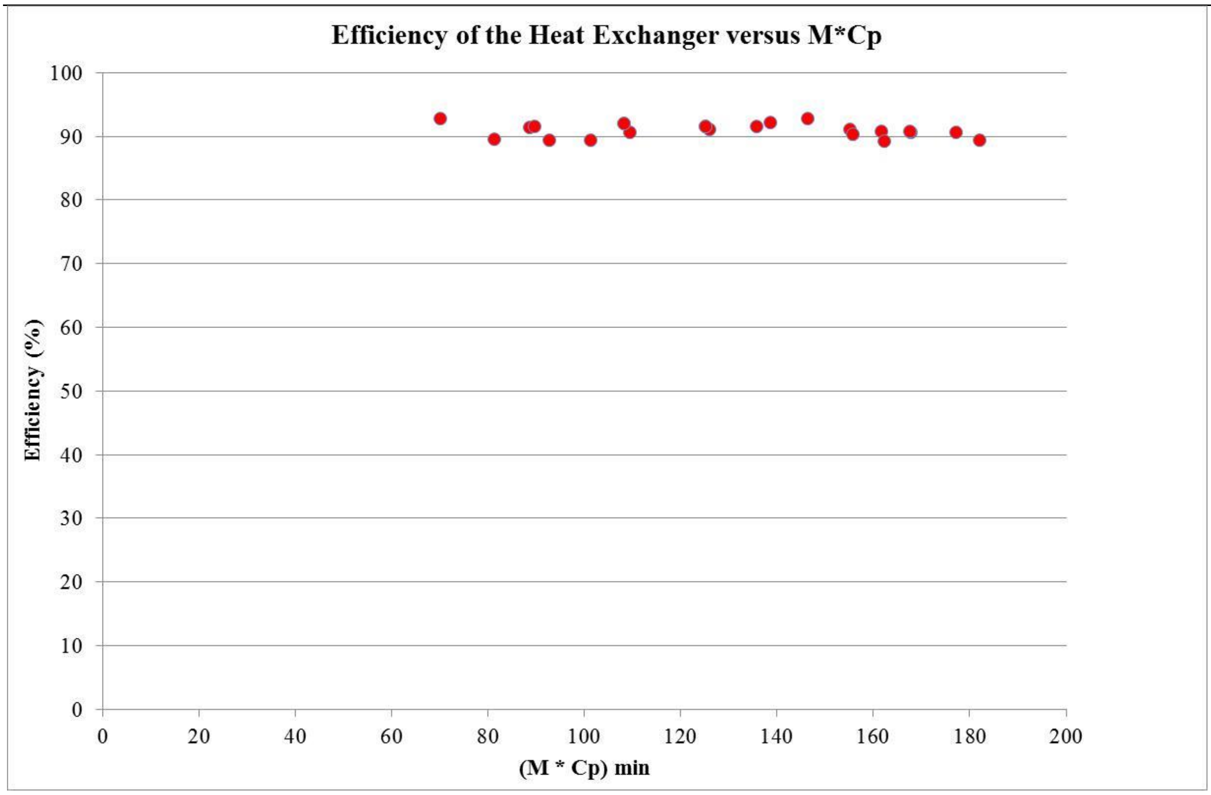

Figure 16 : Efficiency of the Heat Exchanger

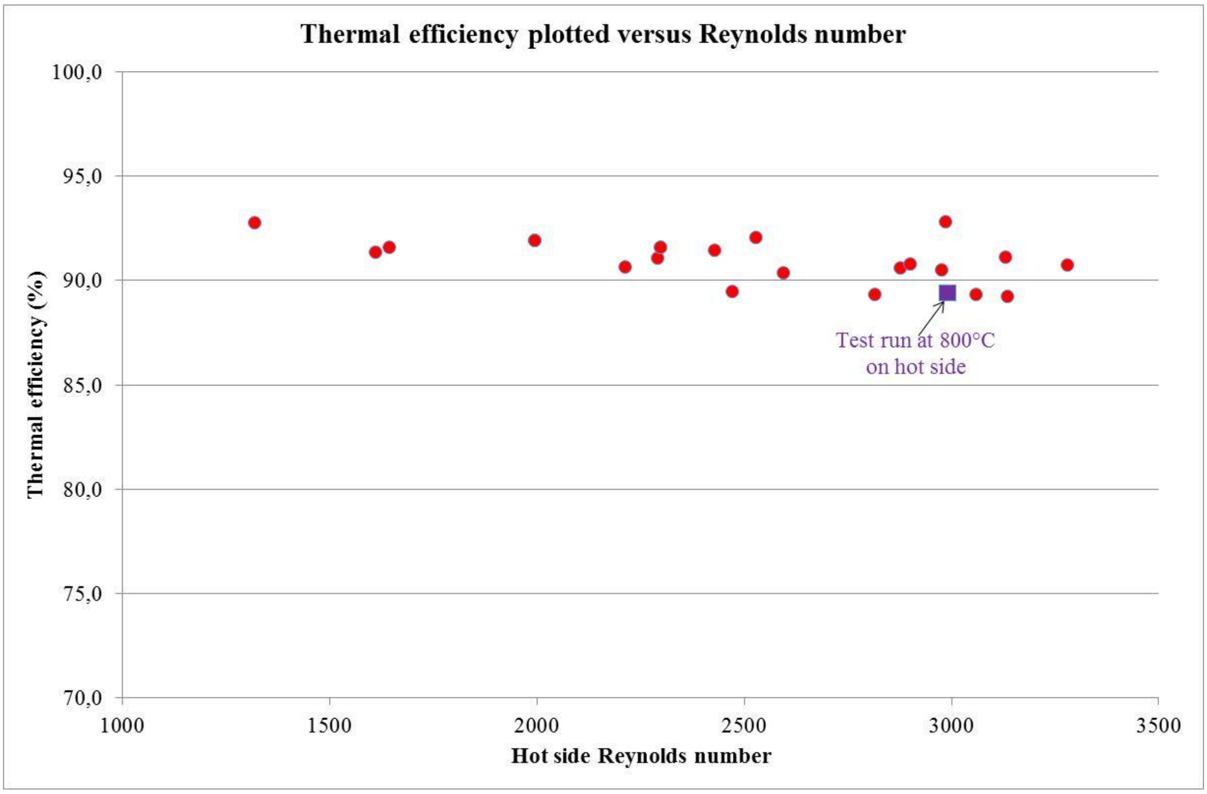

Figure 17 : Efficiency of the Heat Exchanger versus Reynolds number

For the whole range of mass flow rate, figure 16 shows that the thermal efficiency is always higher than 90%. The Claire loop limitations prevent the loop working at higher mass flow rates. Theoretically, thermal efficiency should therefore decrease progressively.
The nominal working conditions used to size the air mock up lead to a theoretical Reynolds number of 3500 but this can't be reached experimentally (low limitation). Nevertheless, as the profile of the plot is relatively flat we can conclude that the global thermal efficiency is quite good.

Figure 15 shows that the thermal performance of the plates is lower than predicted by the CFD calculations. As with the hydraulic calculations, the CFD modelling was undertaken on a pattern made of corrugated plates assuming an ideal case and more especially without bypasses along the longitudinal edges. <u>Further analyses will not result in a change of the thermal performance of the global heat exchanger</u> but will eventually allow checking of the validity of the CFD correlation.

2nd method for taking into account flow bypasses along the longitudinal edges:
As explained in the paragraph dedicated to the hydraulic performance, some of the air doesn't flow inside the active area of the plate but in the gap located along the longitudinal edges.
We estimated the percentage of mass flow bypassing the active part of the plate by considering:

- the size of the gaps;
- the difference of friction factors between gaps and the active part;
- the physical properties on the fluids.

Considering 10% of the air flow inside the bypasses:

- 90% of flow in the active : using the first CFD correlation → $h_{active\ part\ h,c}$ for both fluids
- Calculation of global heat exchange coefficient in active part using :

$$\frac{1}{U} = \frac{1}{h_c} + \frac{1}{h_h} + \frac{e}{\lambda} \qquad (12)$$

- 10% of the flow in the bypasses : using literature correlation → $h_{bypasses\ h,c}$
  Use of Petukhov and Gnielinski correlation:

$$Nu_{by-pass} = 0.0214\left({Re_{Dh}}^{0.8} - 100\right)Pr^{0.4}\left(1 + \left({}^{D_h}/_{L}\right)^{2/3}\right) \qquad (13)$$

- Calculation of global heat exchange coefficient in the bypasses using (12) and *h* $_{h,c}$ for both fluids in the bypasses for (13).

- From the global heat exchange coefficients, the outlet temperature of both fluids is calculated at the outside of the active area and for the bypasses.

- Mixed temperatures are calculated for both fluids :

$$T\ mixed_{\ h,c} = \left[\frac{(Mtot * 0.9 * T)_{active\ area} + (Mtot * 0.1 * T)_{bypasses}}{Mtot}\right]_{h,c}$$

- Mixed temperatures are compared to experimental measurements and $h_{active\ part\ h,c}$ (initially determined using CFD correlation) are corrected to obtain experimental measurements.

This correction of the bypass effects enables the determination of the thermal behavior of the stamped plates and can be directly compared to the CFD results.

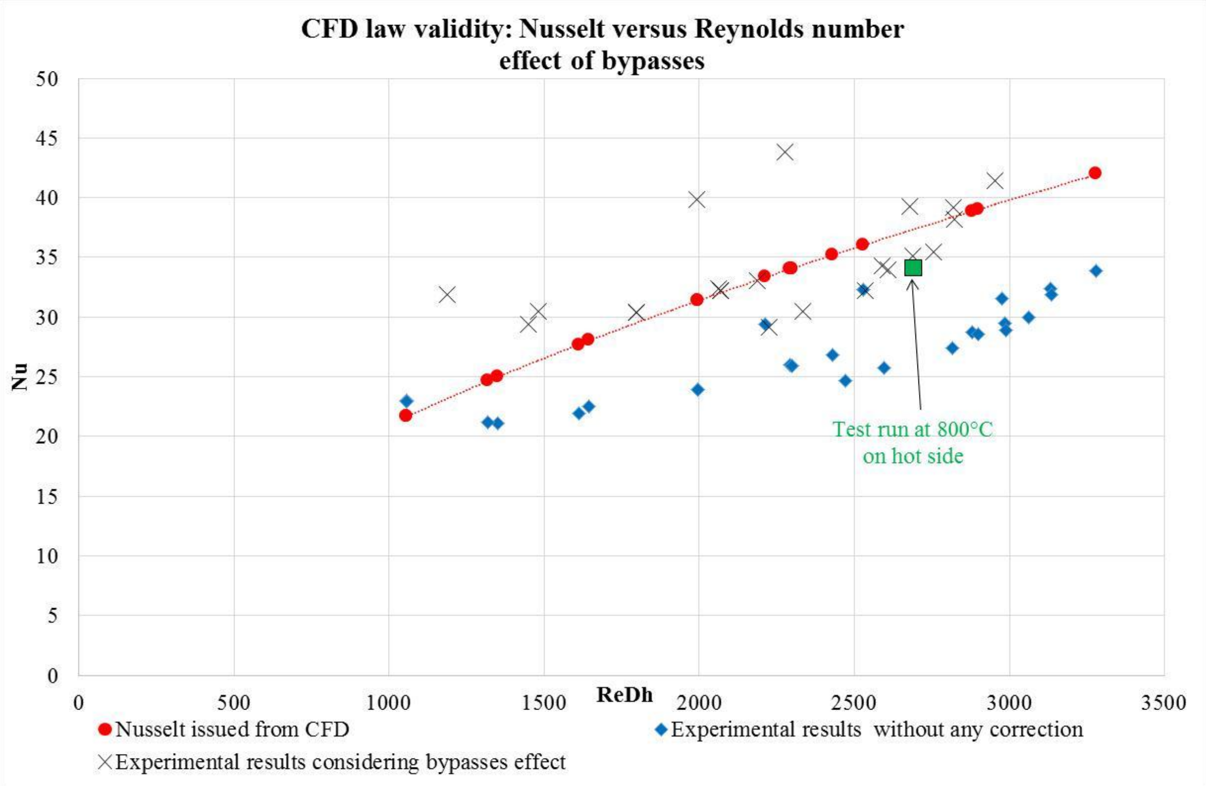

Figure 18 : Effect of bypasses – final thermal performances

Figure 18 shows clearly the effect of the bypasses on the thermal performance of the stamped plates: experimental tests lead to data quite closed to the CFD predictions. Despite some dispersion between experimental results, the thermal performance of the plate is quite well described by the CFD law and the correlation can be reliably used to size the technology. We must be aware however that a part of the fluid flows through the bypasses and this has to be taken into account during sizing or with regard to the technical aspects: for example by proposing a device to limit this flow.

5. THERMO MECHANICAL TESTS

Thermal shocks have to be applied to the heat exchanger but they have to be carefully controlled to prevent early damage. The procedure is adopted as follows:

- from the thermal steady state the hot temperature are suddenly decreased by a given temperature variation;
- a new pseudo steady state is reached such that the internal HX temperatures have enough time to decrease to this “steady state”;

- the hot inlet temperature returns to its initial value.

It was decided to increase progressively hot inlet temperature and also temperature variation. The final goal is to reach the following temperature profile at the end of the test campaign.

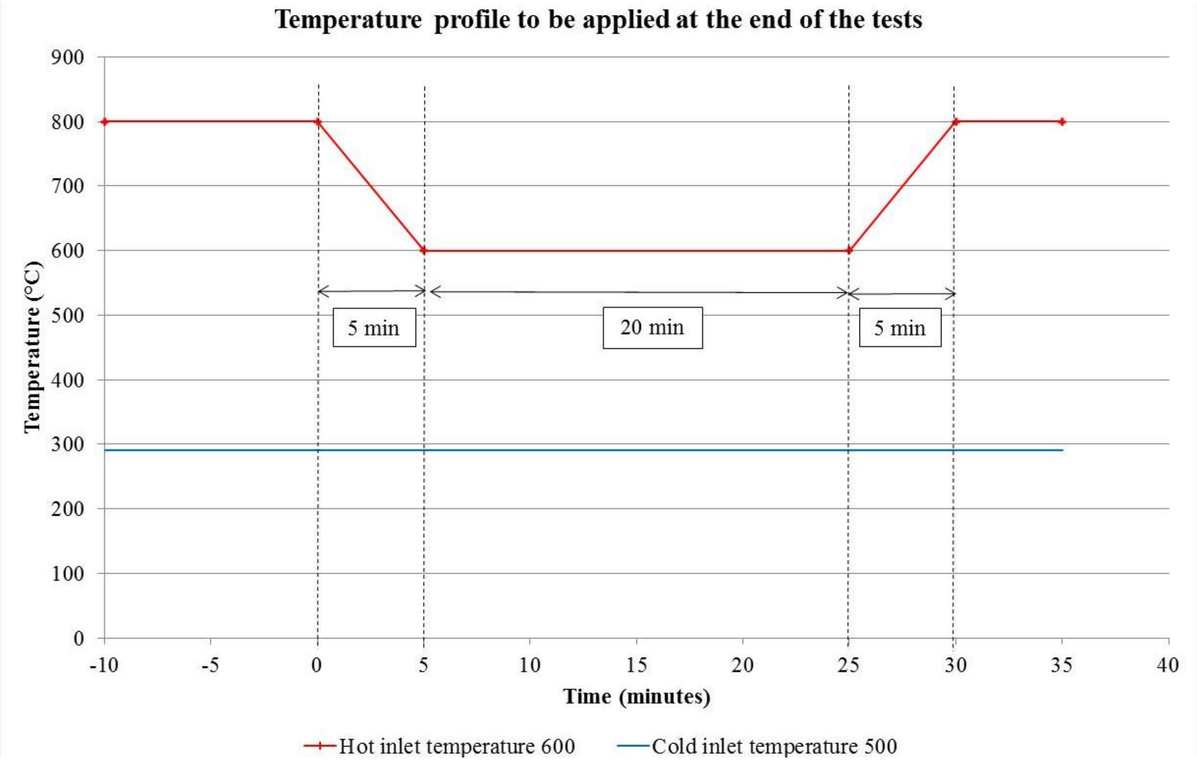

Figure 19 : Final expected temperature profile to be applied at the end of the campaign during thermal shocks

Table 4 reminds the initial agenda of tests when increasing progressively the level of temperature.

Hot inlet temperature	Hot inlet temperature variation	Time duration of the campaign	Number of shocks
650°C	100°C	1 week	As many as possible
	150°C	1 week	ditto
	200°C	1 week	ditto
Helium leak detection			
700°C	200°C	1 week	ditto
Helium leak detection			
750°C	200°C	1 month	~ 1 / week
Helium leak detection			
800°C	200°C	1 month	~ 1 / week
Helium leak detection			

Cold inlet temperature is kept constant = 290°C
Table 4: Recall of agenda of tests

The following figures (in section 5.1) present the temperature measurements obtained at the inlet and outlet of the Heat exchanger during the thermal transient and table 5 sums up the effective number of thermal shocks.

Hot inlet temperature	Hot inlet temperature variation	Effective time duration of the campaign	Number of shocks
650°C	100°C	1 week	30
	150°C	1 week	40
	200°C	1 week	54
700°C	200°C	1 week	31
750°C	200°C	1 month	11
800°C	200°C	1 month 1/2	4

Table 5: Effective number of thermal transients

5.1 Presentation of the results during transient

This section presents the graphical results of the tests described in table 5. Generally inlet and outlet temperatures and flow rates on both sides are plotted as a function of time.

Emphasis is placed on checking the agreement with theoretical specification (comparison with figure 19) and comparing the first and the last shocks of one campaign.

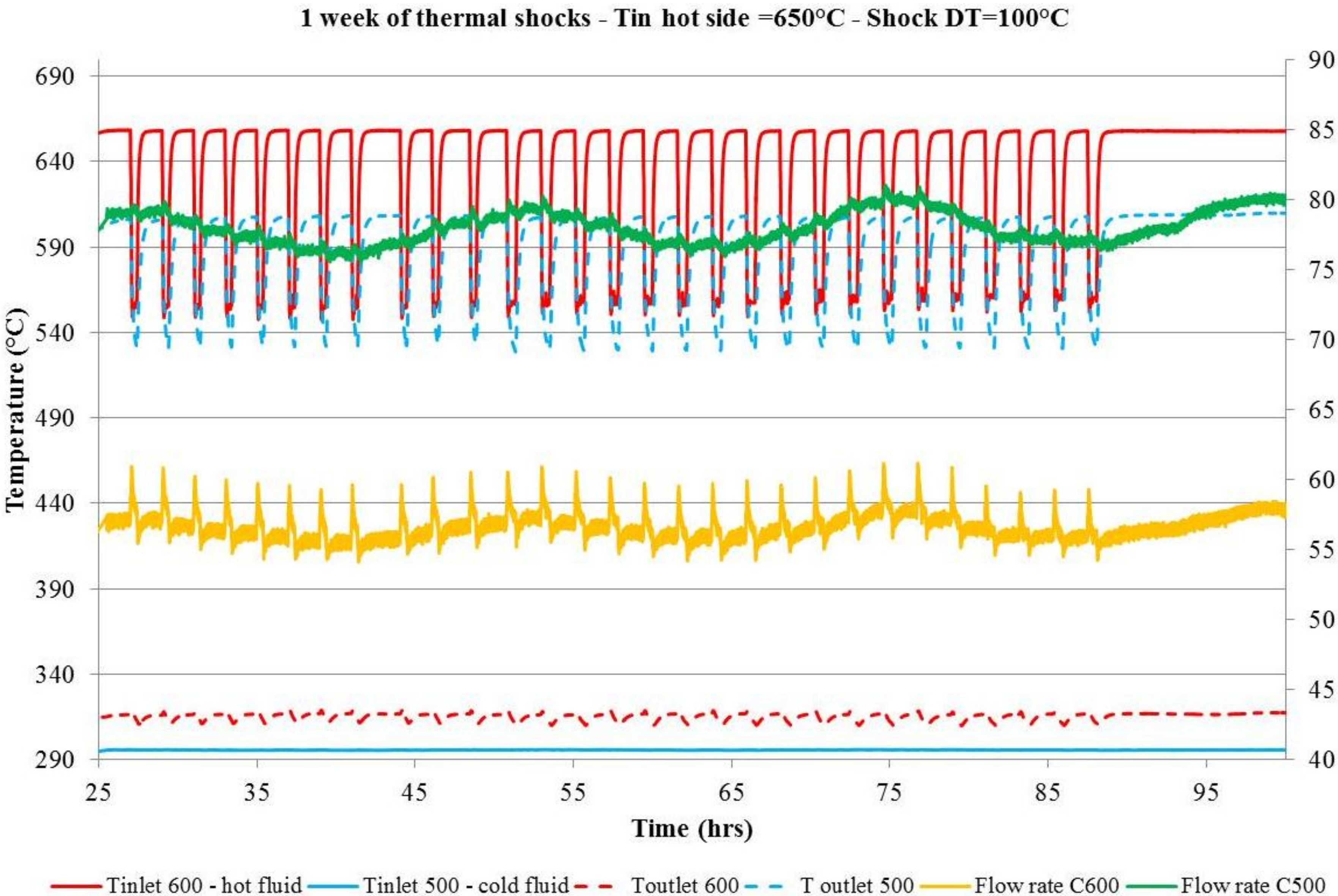

Figure 20 : 1 week of thermal shocks Tin = 700°C – DT =200°C

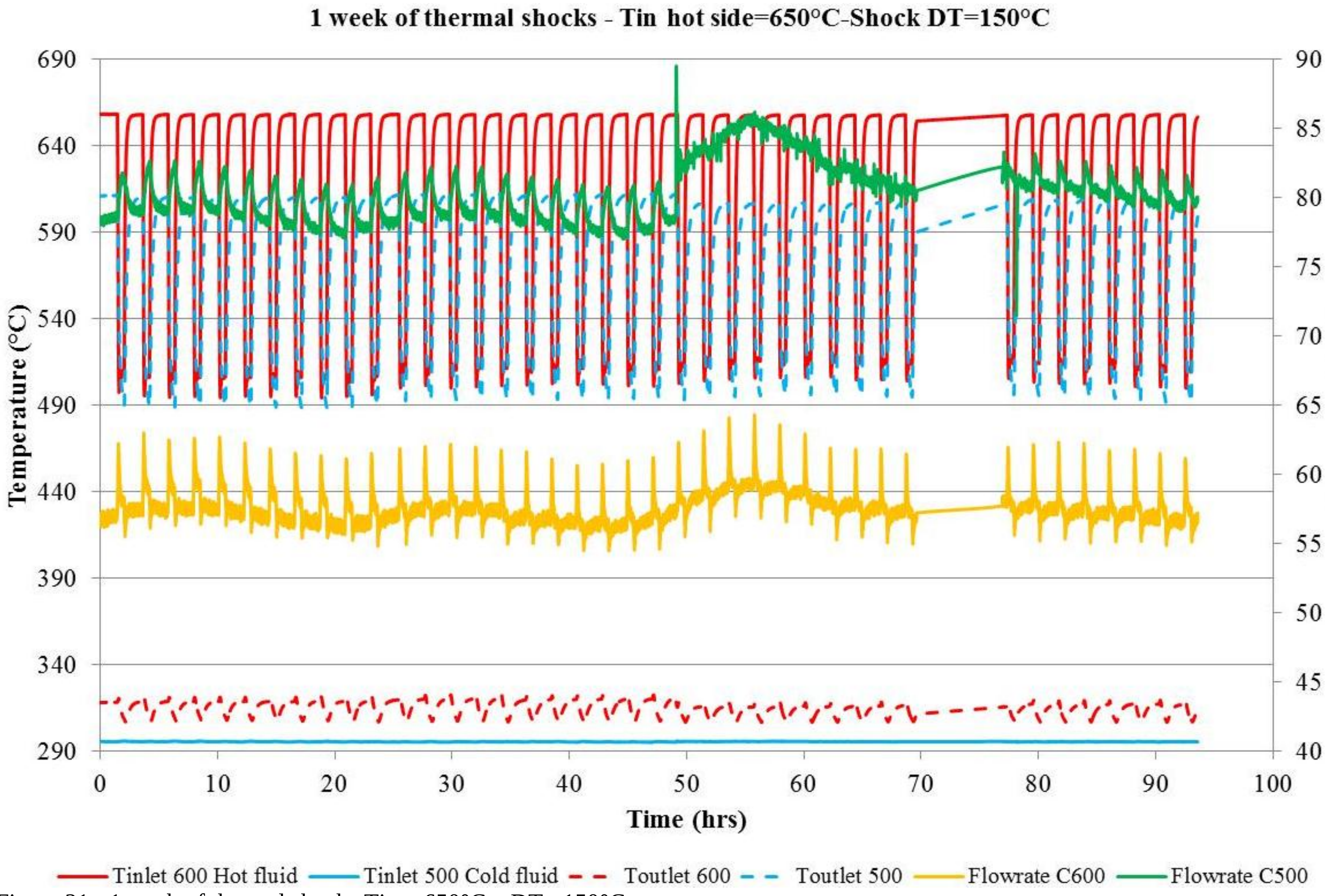

Figure 21 : 1 week of thermal shocks Tin = 650°C – DT =150°C

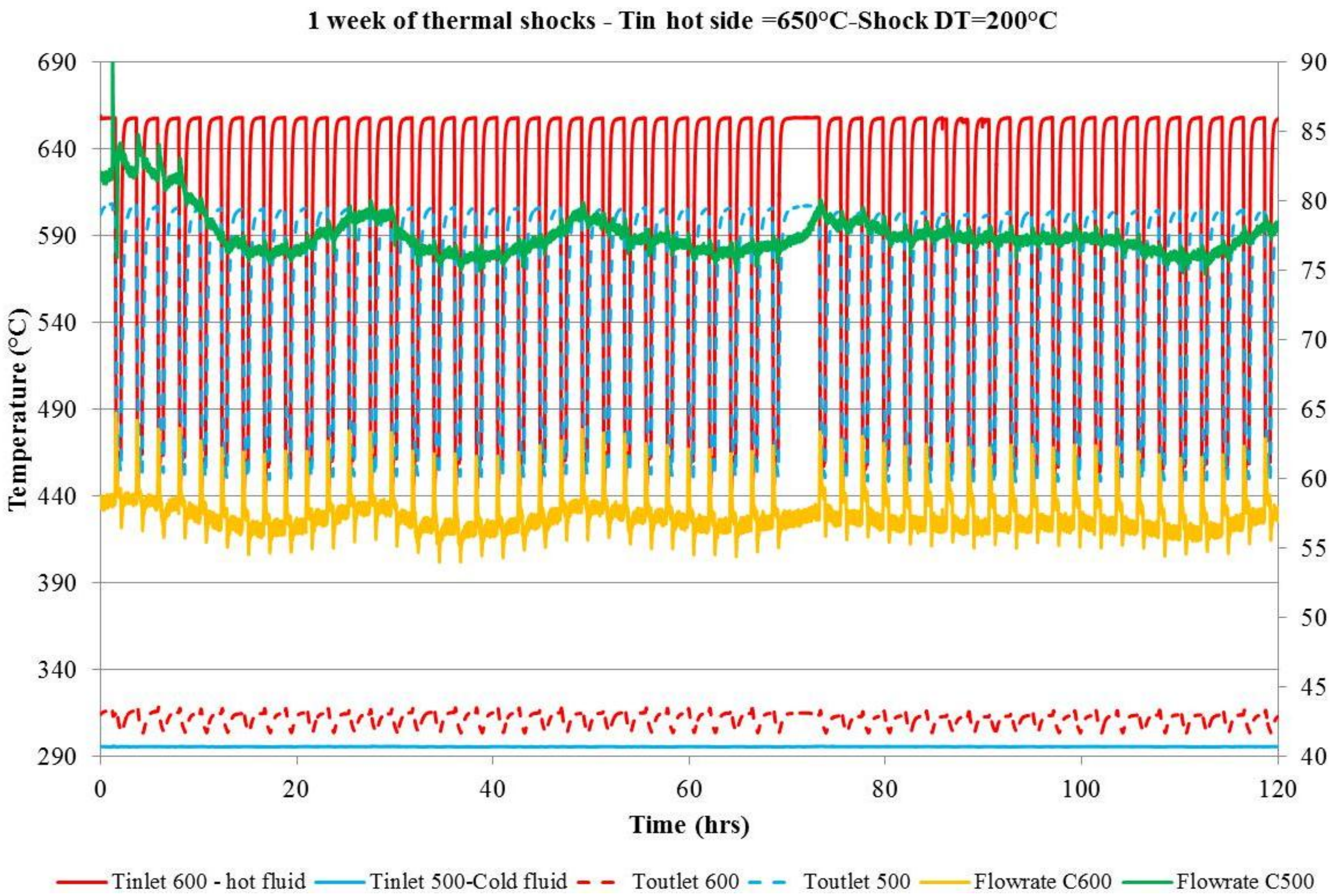

Figure 22 : 1 week of thermal shocks Tin = 650°C – DT =250°C

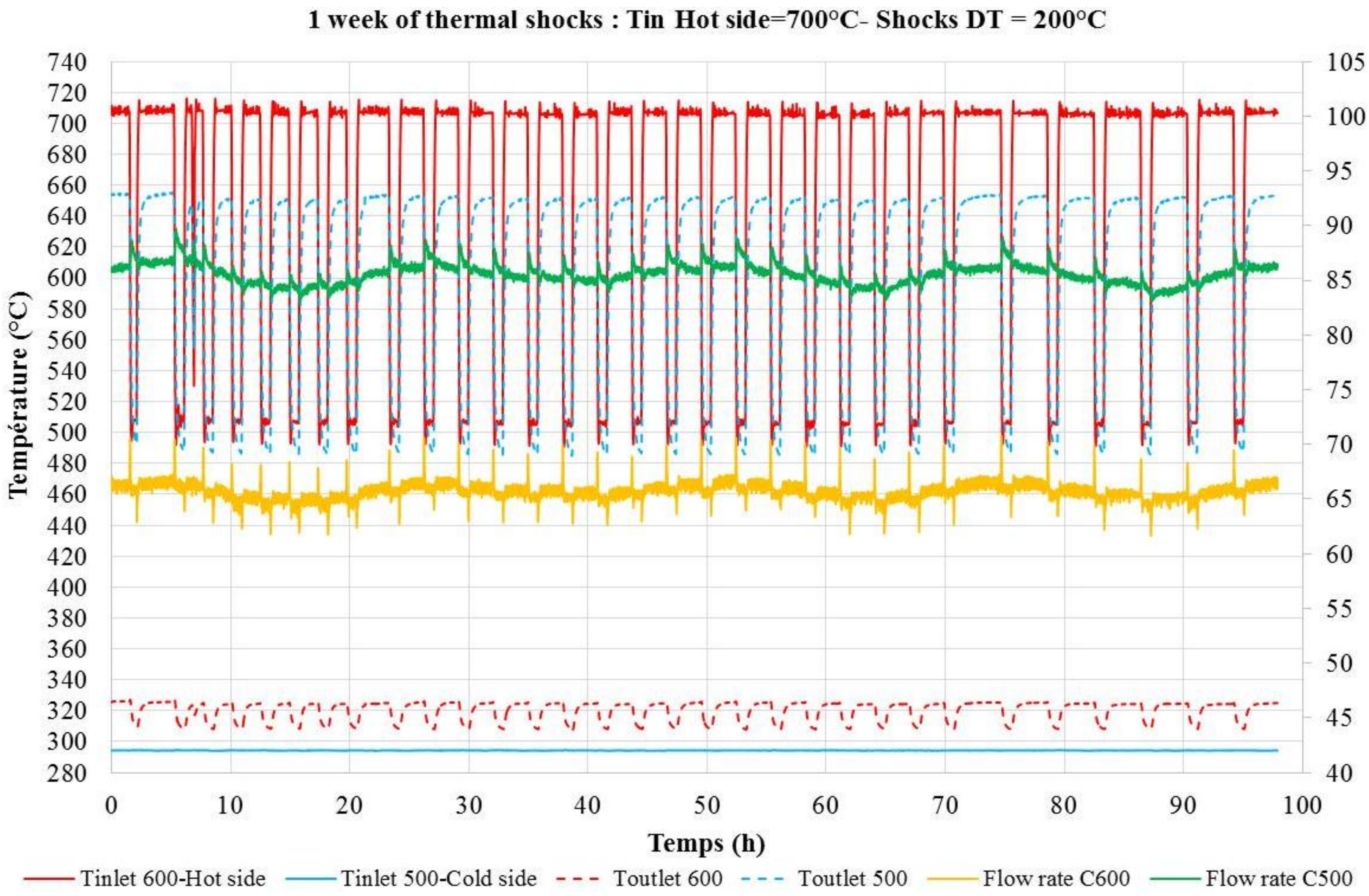

Figure 23 : 1 week of thermal shocks Tin = 700°C – DT =200°C

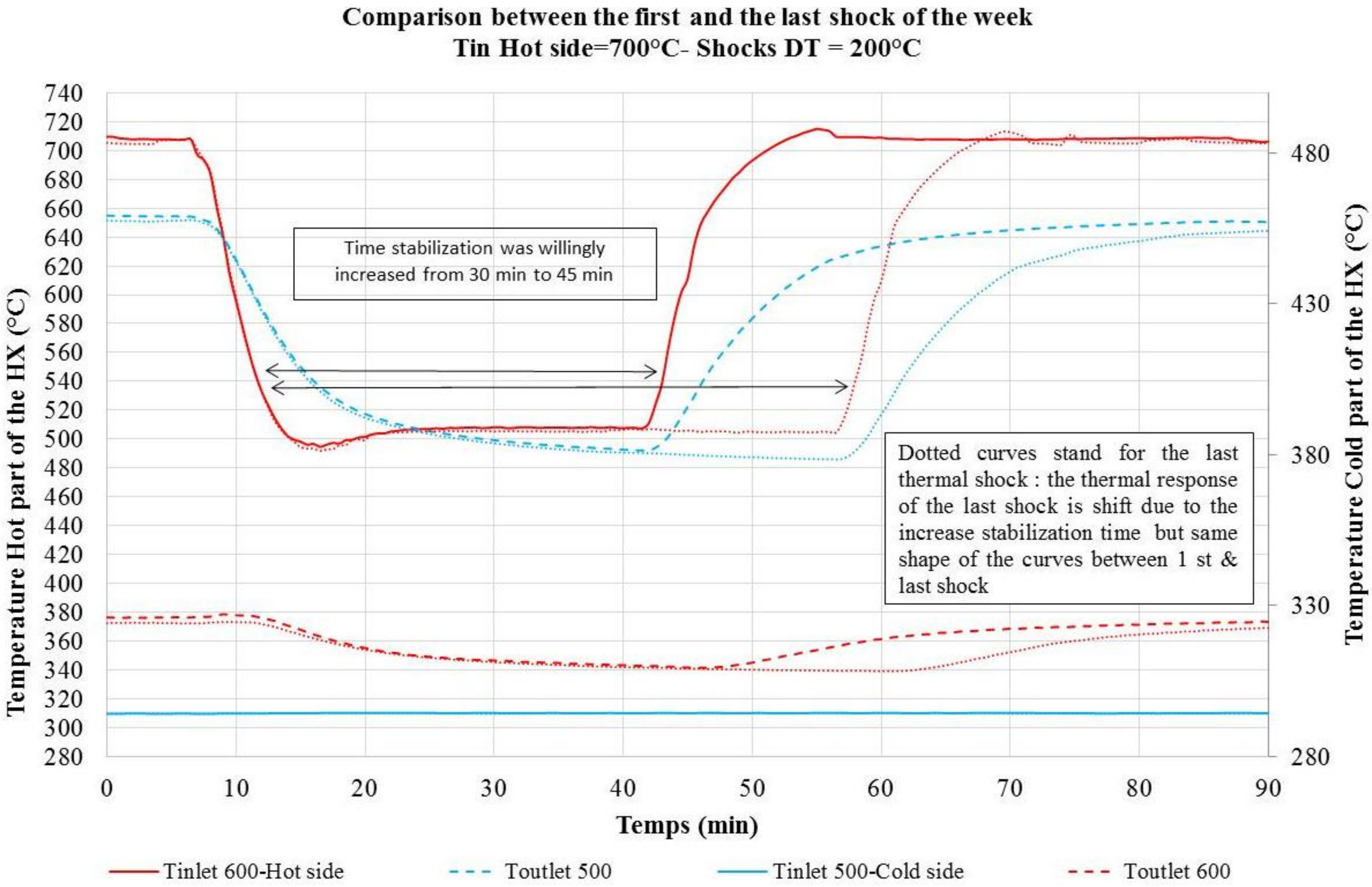

Figure 24 : Comparison between the first and the last shock of the week - Tin = 700°C – DT =200°C

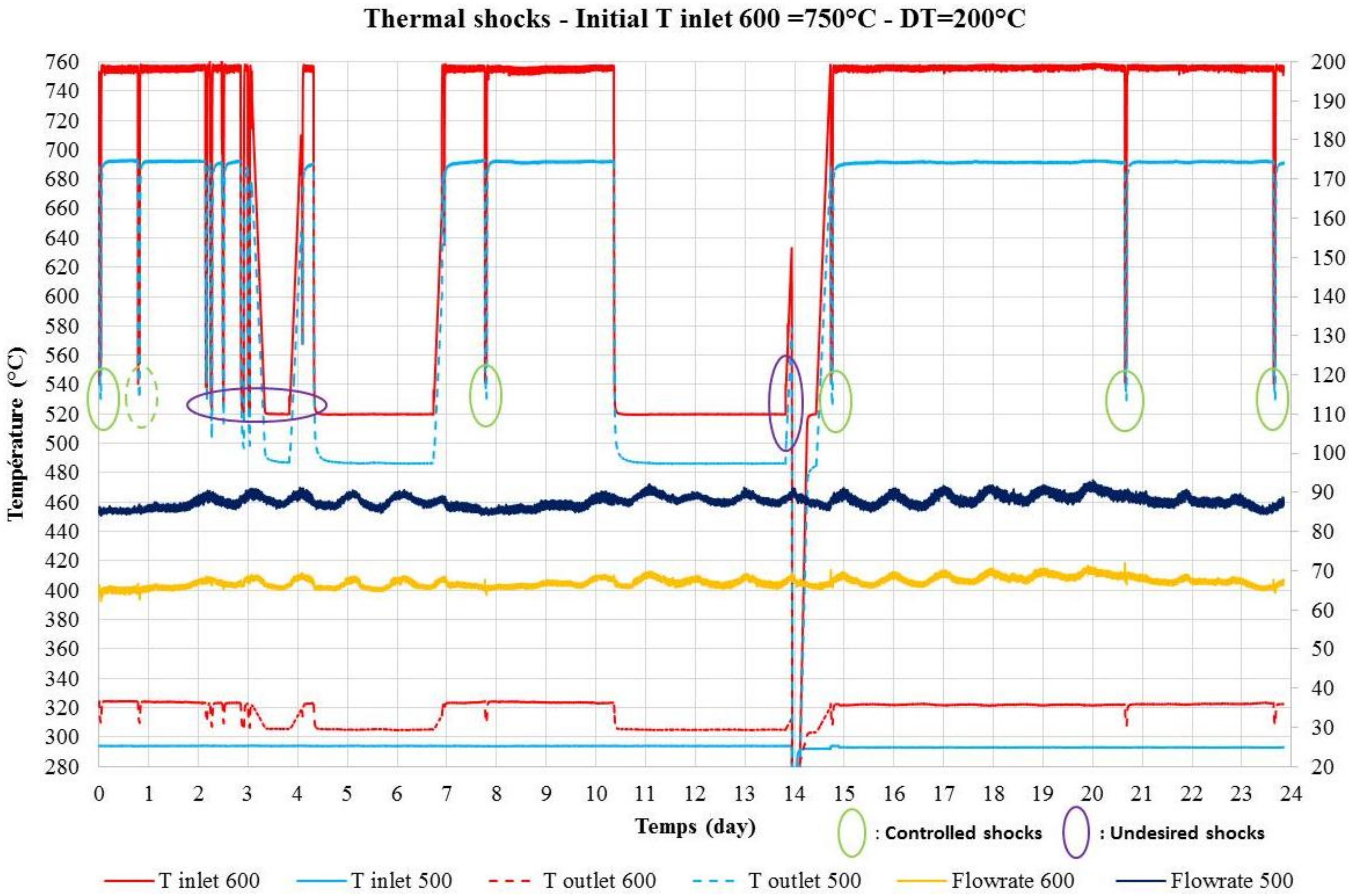

Figure 25 : 1 month of thermal shocks Tin = 750°C – DT =200°C

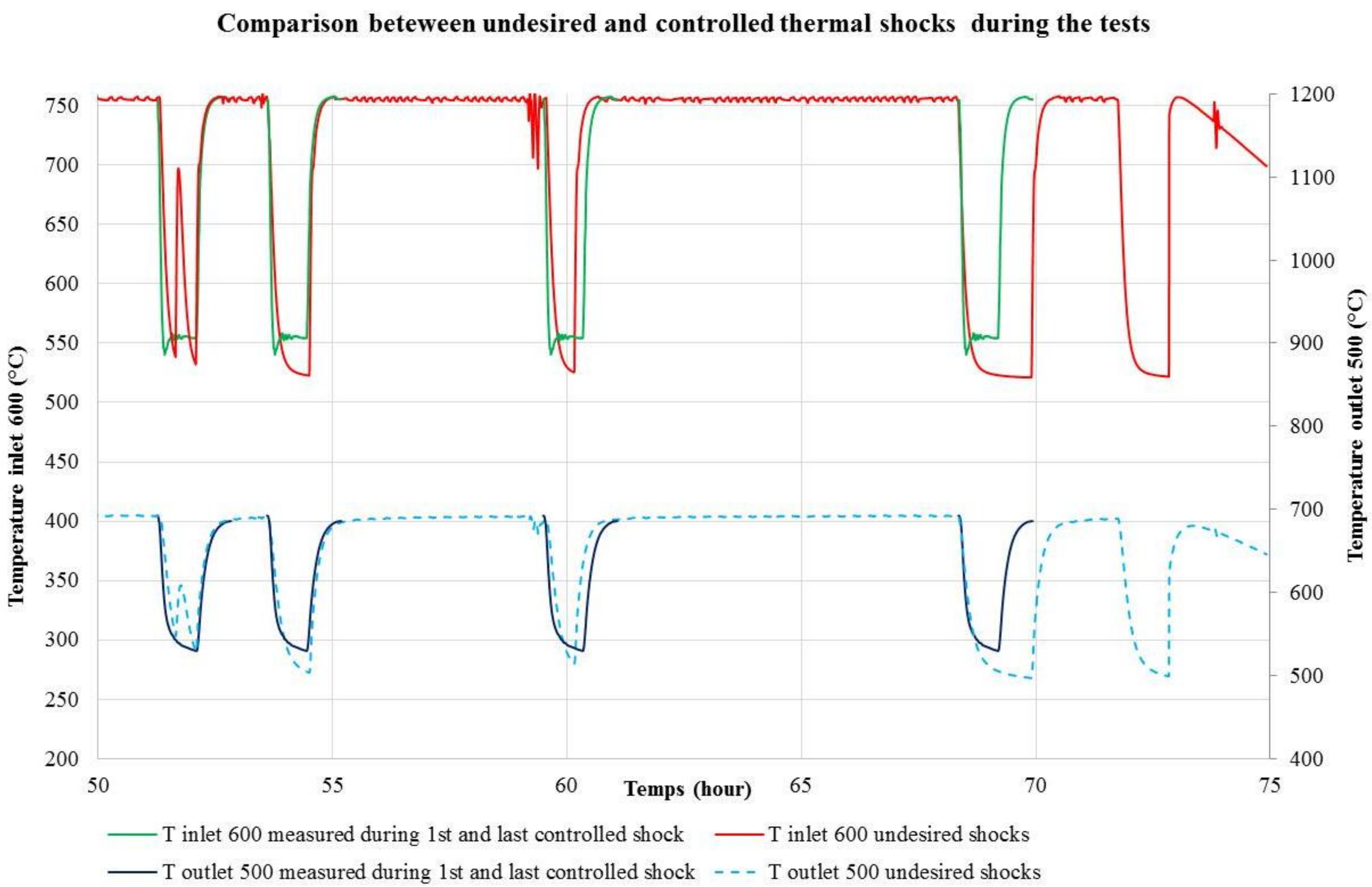

Figure 26 : Comparison between desired and undesired thermal shocks (Tin = 750°C – DT =200°C)

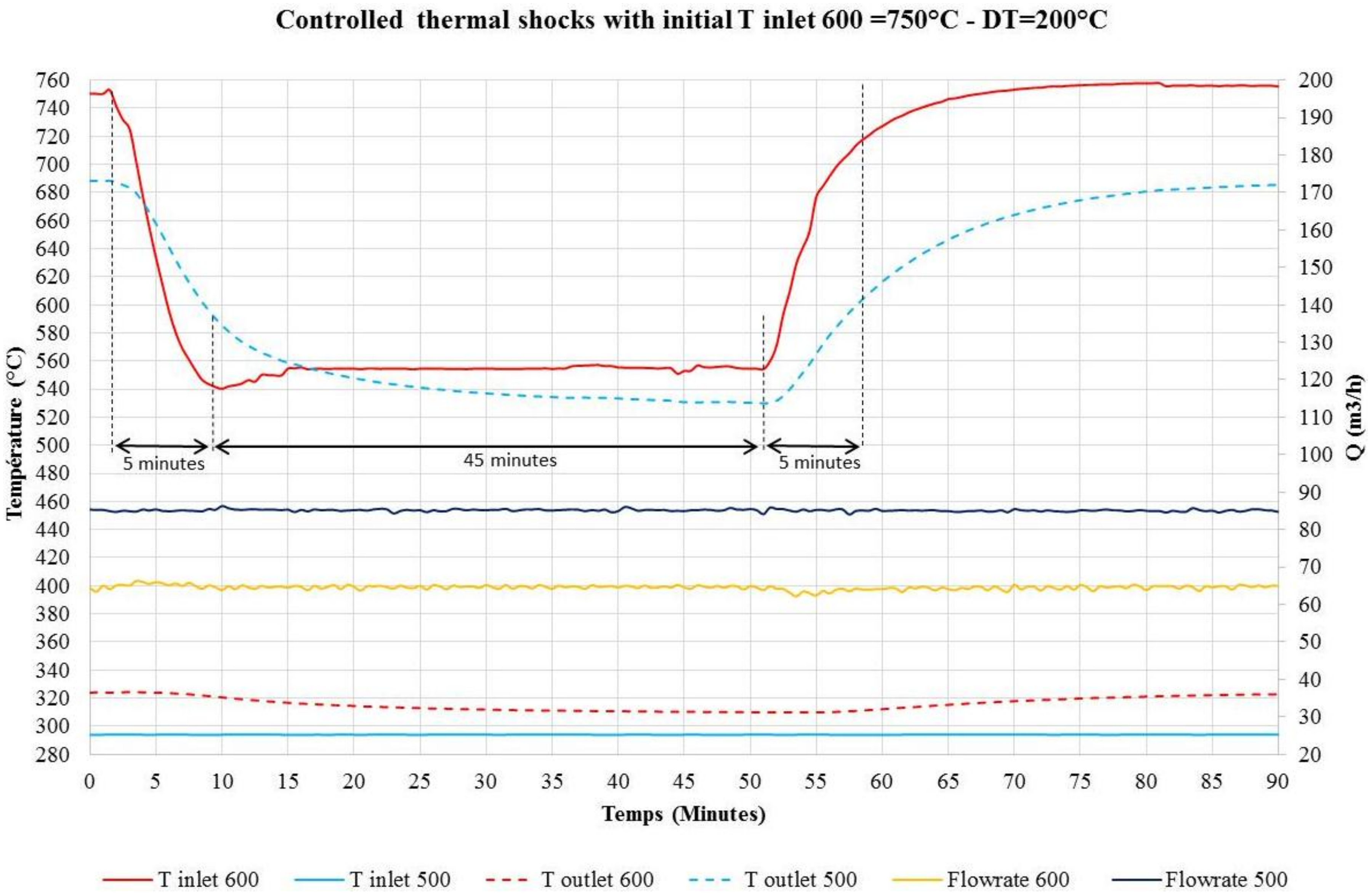

Figure 27 : Detail of a thermal shock (Tin = 750°C – DT =200°C)

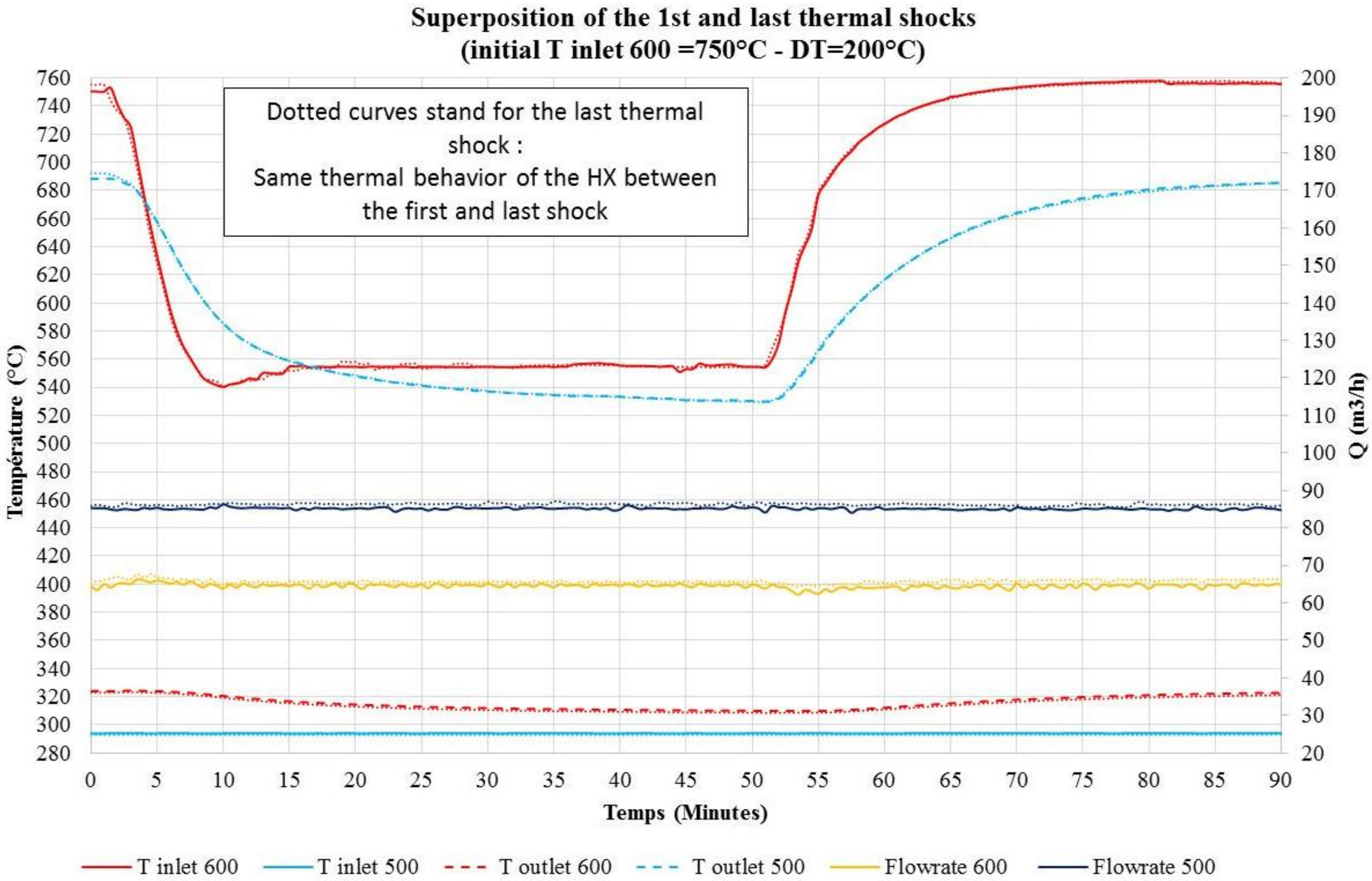

Figure 28 : Superposition of the first and last thermal shocks (Tin = 750°C – DT =200°C)

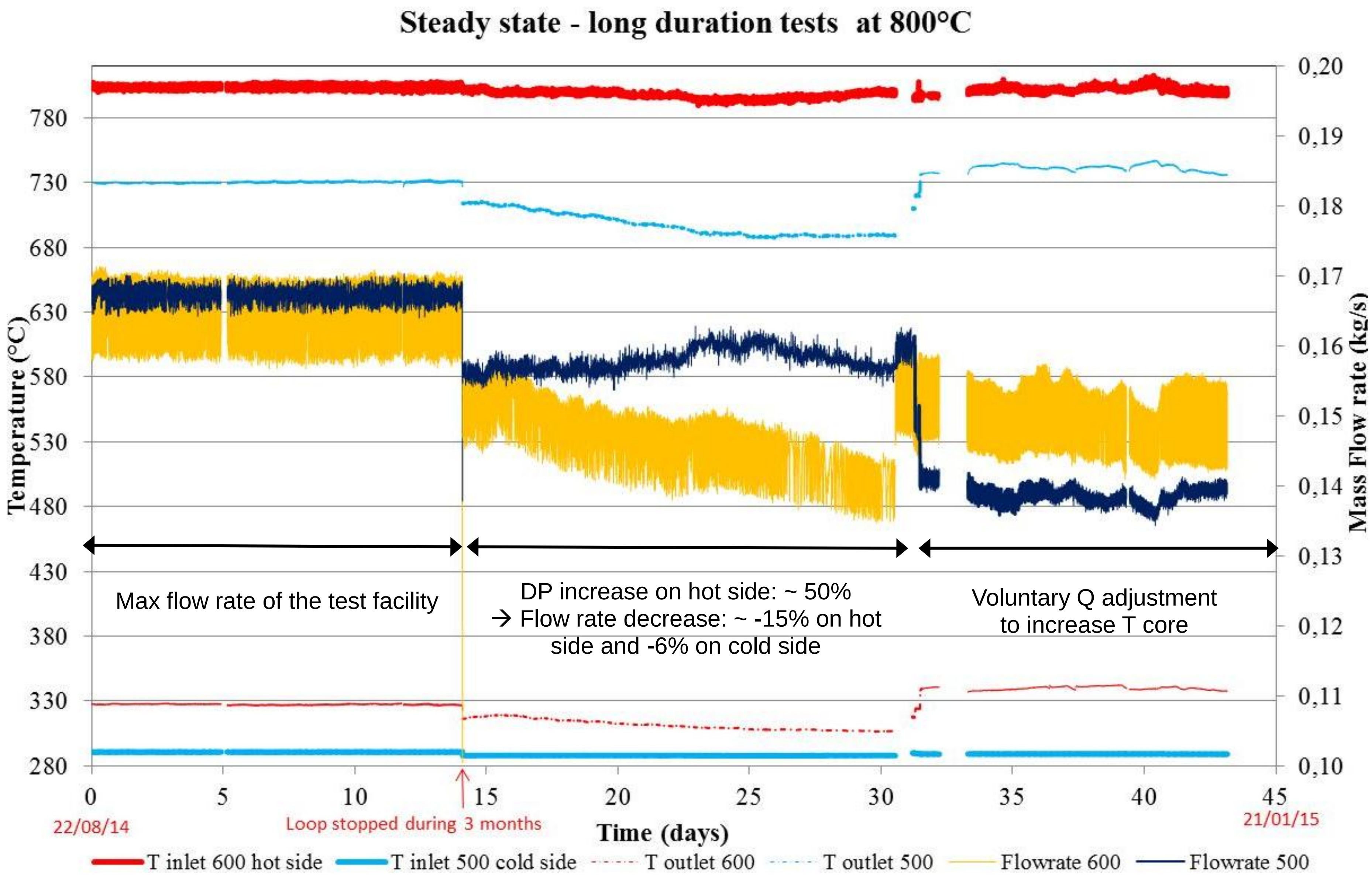

Figure 29 : Steady state – long duration tests at 800°C

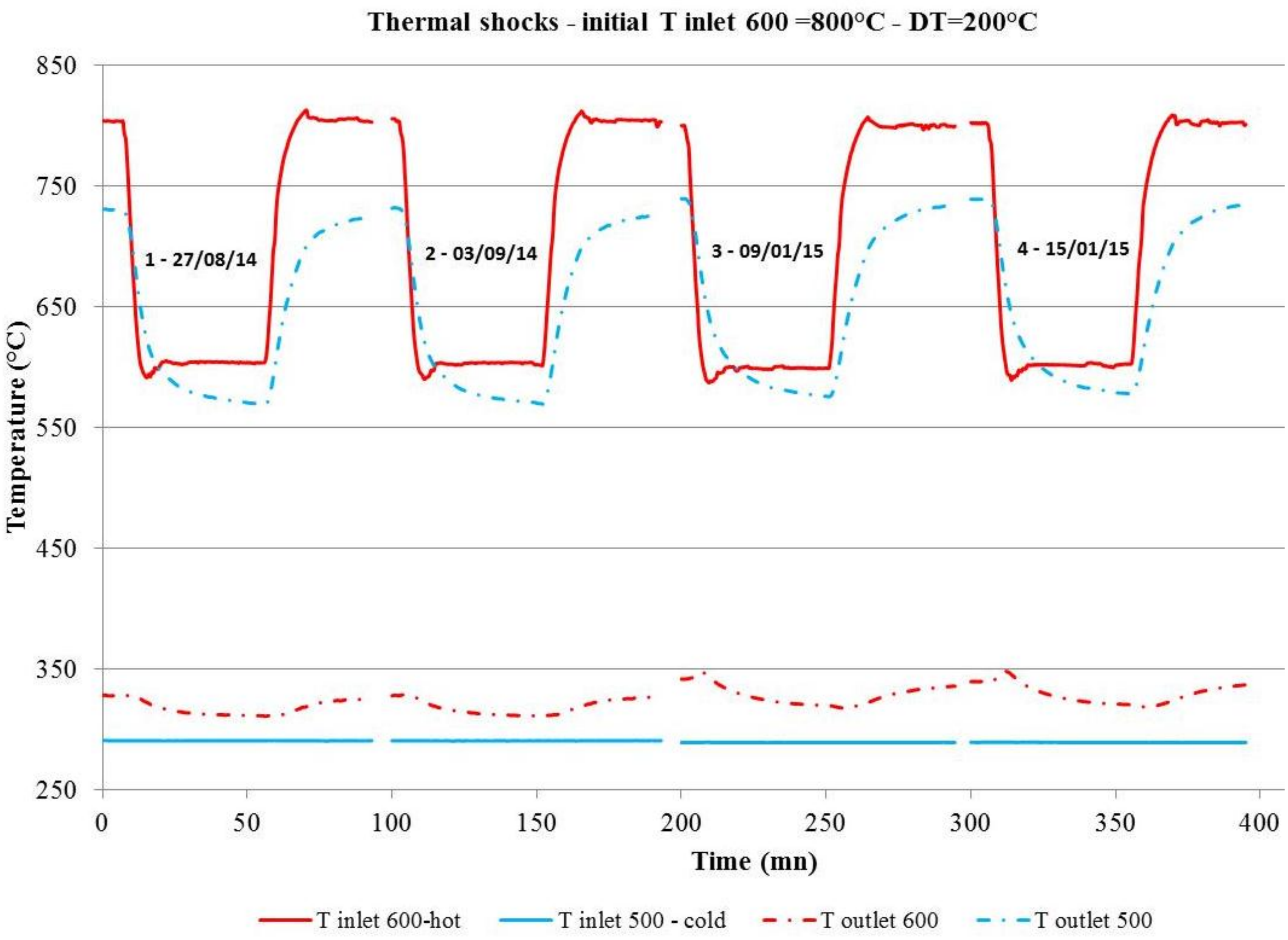

Figure 30 : Thermal shocks at 800°C

In the previous report, 12 days of tests were in steady state at 800°C. Few days after, a fire ignition occurred in an electric box leading to the damage of the largest heater. Almost 3 months were required to restart the test facility since it is a very specific product. Figure 29 shows a slight decrease of the flow rates: -15% on hot side and -6% on cold side. The flow rate decrease is directly linked to an increase of pressure drop on hot side of the heat exchanger. This increase of pressure drop occurred immediately after the loop was restarted: either something is in front of the hot inlet channel or oxidation clogs partially the channels. Global performance is not affected and therefore tests went on, by adjusting a higher hot flow rate than cold one to increase willingly the metal temperature mainly of hot part of the heat exchanger.

6. COMPARISONS WITH CFD RESULTS

CFD calculations were run to extract the thermal behavior of the mock up and to provide temperature fields to run the FEM calculations.

CFD simulations were carried out on single plate geometry and on a part of the stack with a thick end plate.

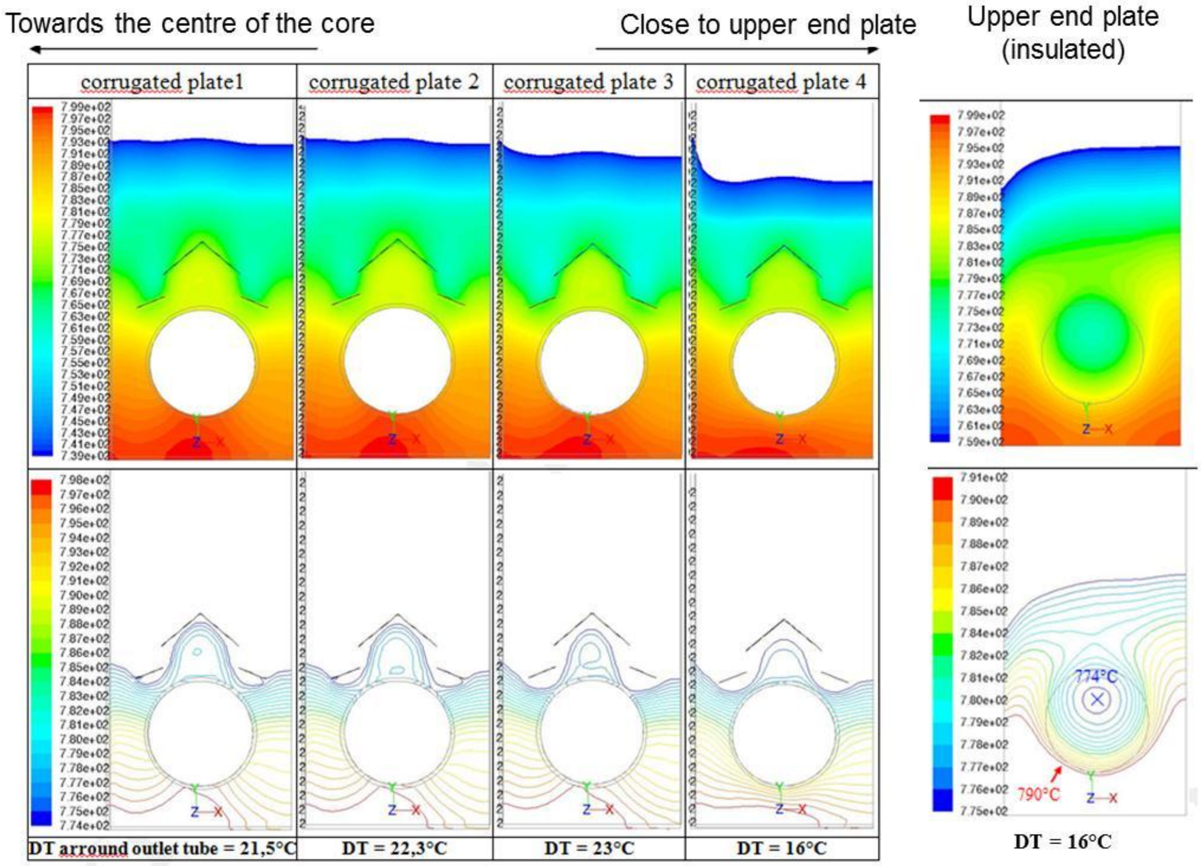

Figure 31 : Temperature fields issued from the CFD calculations

These results were obtained assuming a perfect thermal insulation on the outside surfaces of the plate bundle. From experimental measurements, it is possible to make comparisons with these calculations.

The next figures show the location of external temperature probe and provide comparisons of the temperatures.

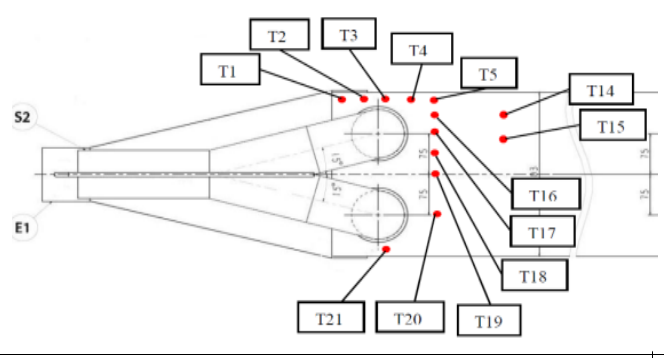

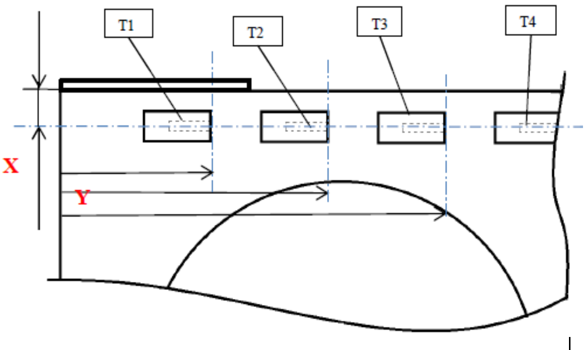

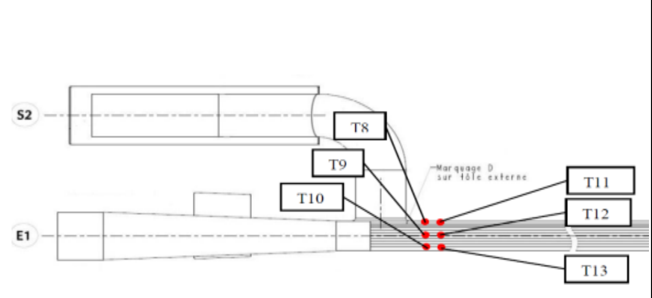

Upper outer plate

	X (mm)	Y(mm)
T1	17	20
T2	17	52.5
T3	17	85
T4	17	117.5
T5	17	150
T16	46.5	150
T17	76.5	150
T18	114	150
T19	151.5	150
T20	226.5	150
T21	286	85

21 thermocouples are located on the core :

- 13 are on the same side (upper end plate)
- 6 are along the height of the stack
- 2 are on the lower end plate : T6 and T7 – opposite position to T 5 and T17

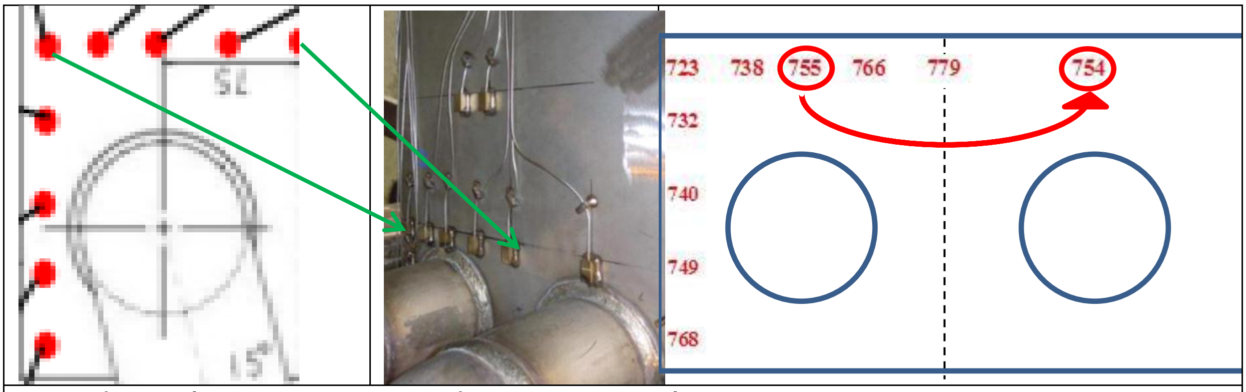

Experimental measurements on the upper outer plate

T16 and T20 gives the same temperature → Good transverse flow distribution

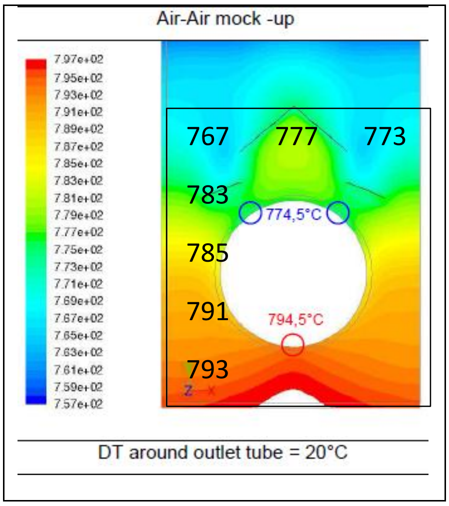	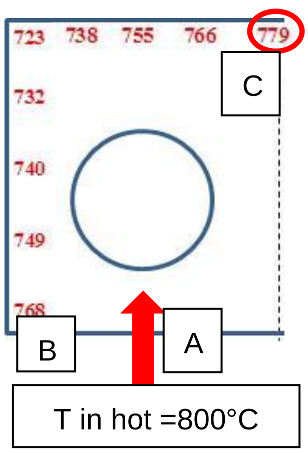	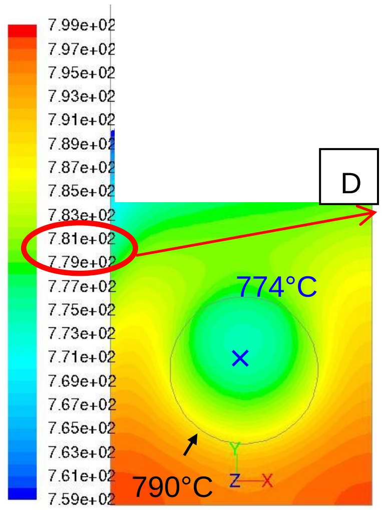
Results from CFD simulation – **internal** plates	T Measurements of the **end** plate	Results from CFD simulation – **end** plate

Comparisons are made between measurements and CFD simulations run on the mock up. Comparisons must be carefully made since measurements are located outside of the plate bundle (on the end plate) and can't be directly compared to CFD calculations within the internal plates.

- At the inlet of the hot part of the heat exchanger, the measured air temperature is 800°C (point A)

- On left side of the distributing area (point B), the metal temperature is quite low compared to the air inlet one: 768°C against 800°C (and is also quite low compared to the CFD result : at the bottom left corner of CFD results T ~ 800°)

- Along the dashed line at the end of the distributing area (point C), the temperature is quite high, i.e. 779°C which is in good agreement with calculation run on the end plate (T (point D) same location : ~780°C).

In the middle of the plate, it is assumed that the expected level of temperature is reached but it is not the case along the edge. It is likely that the thermal losses affect this area: the plate bundle is inserted in the shell and insulation is insured by filling the shell with mineral products and an outer insulation is added outside of the shell. Due to specific shapes of the pipes the bundle is not at the center of the shell (figure 32) and thermal insulation is not optimized.

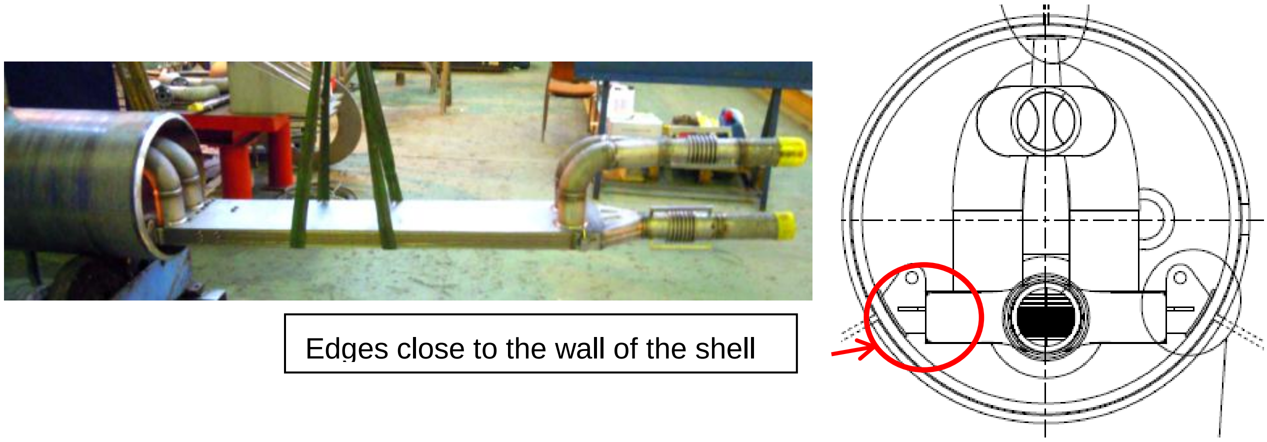

Figure 32 : Location of the bundle in the shell

This hypothesis on the different thermal insulation effects between one point to the other can be checked by looking at other thermocouples: T5 and T17 located on the upper end plate can be compared with those located at the same position on the lower end plate.

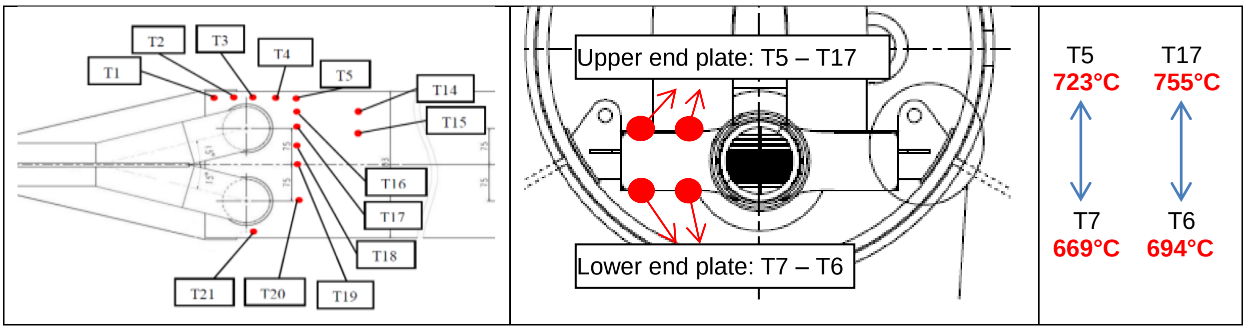

Comparison of temperatures between upper and lower end plates shows an important difference between thermocouples which should roughly indicate the same temperature:

- 723 – 669°C =54°C of difference between T5 and T7
- 755 – 694°C = 59°C of difference between T17 and T6

This difference in boundary conditions is also confirmed when looking at thermocouples located on the longitudinal wall of the bundle.

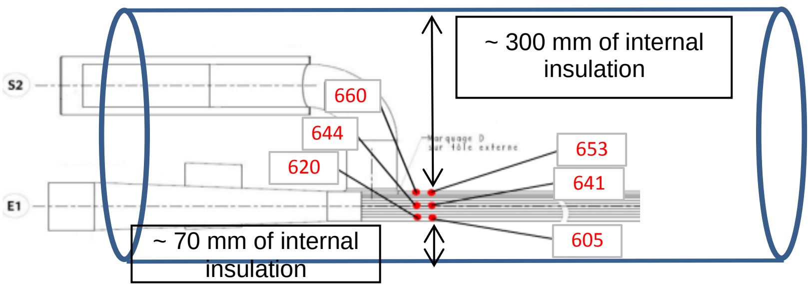

Along the height of the stack of plates, the same order of temperature difference is measured between the top and the bottom.

These local differences of temperature suggest that <u>thermal gradient around the pipes may be different to those obtained by the CFD calculations</u>.

By generating mass flow rate disequilibrium between the hot and cold sides at the end of the test campaign, we intend to modify the map of the plate temperature.

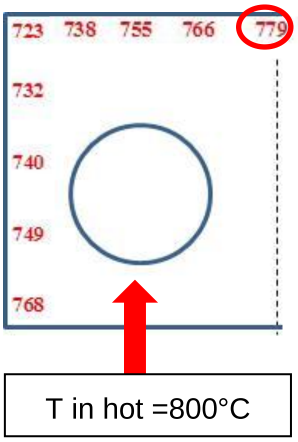

Initial T measurements of the **end** plate

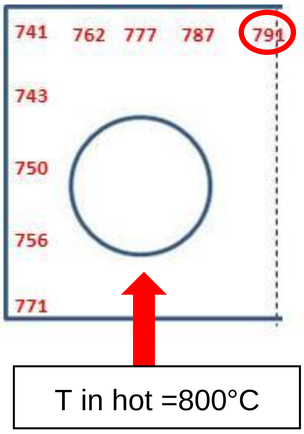

Final T measurements of the **end** plate

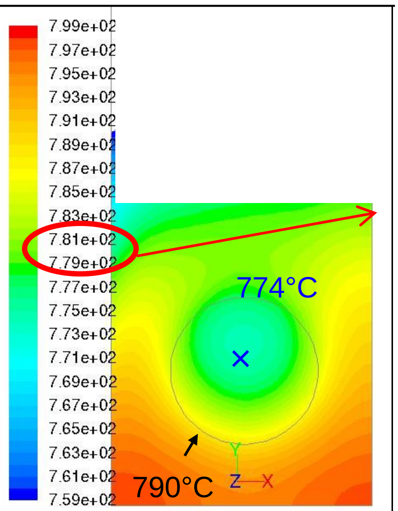

Results from CFD simulation – **end** plate

We still have a transverse temperature difference of around 50°C to be compared to a few degrees predicted by the CFD calculations. We cannot generate a metal temperature of around 800°C near the inlet and the hot air temperature can't no more be increased since the maximum thermal performance of the test facility has been reached.

On figure 33, the fluid temperatures in the hot part of the heat exchanger have been plotted. CFD calculations and experimental data are compared when a thermal shock is applied. It is reminded that it was decided to keep the hot temperature constant for a longer time before going back to 800°C which is the reason why the thermal behavior is different between the CFD results and measurements when t =1500s.

The thermal response is well described globally by the CFD calculations but since the global efficiency of the heat exchanger is lower than the expected one, the initial experimental air outlet temperature (t=0s) is lower than the predicted one. This phenomenon may also impact on the mean metal temperature which tends to be lower for the measurements than for the CFD prediction.

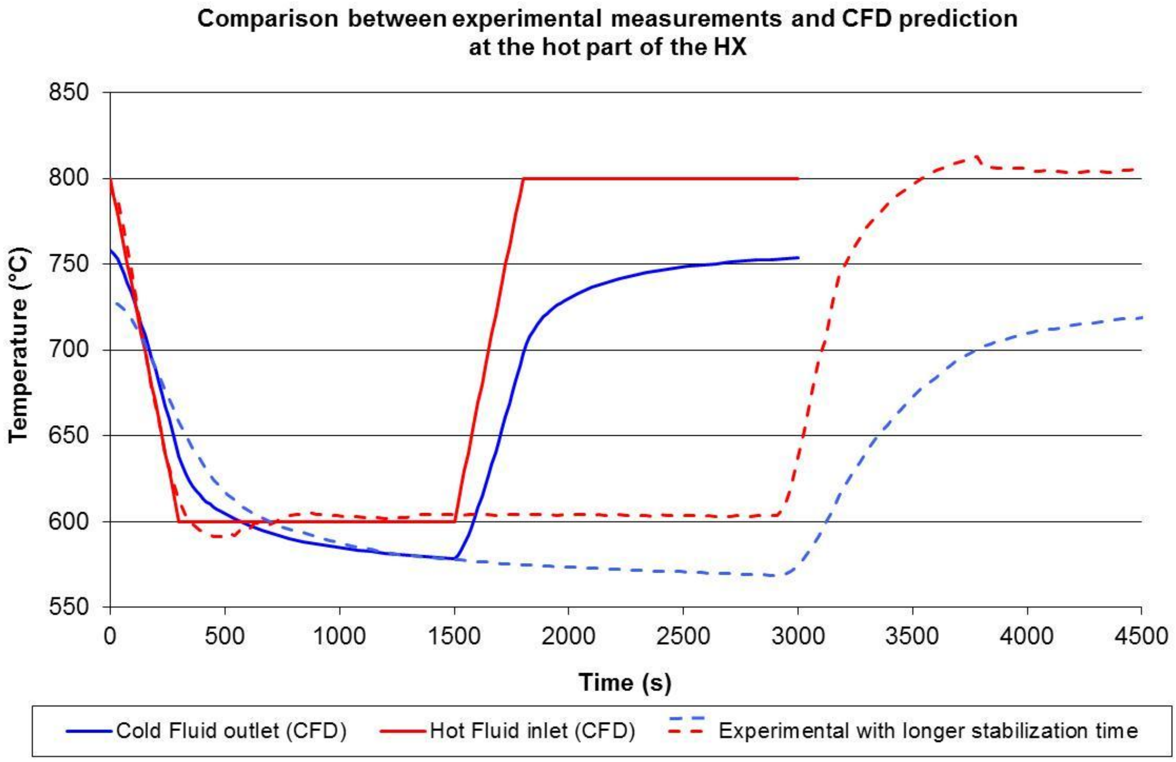

Figure 33 : Comparison of air temperatures at hot part of the HX between CFD and measurements

7. LEAK DETECTION

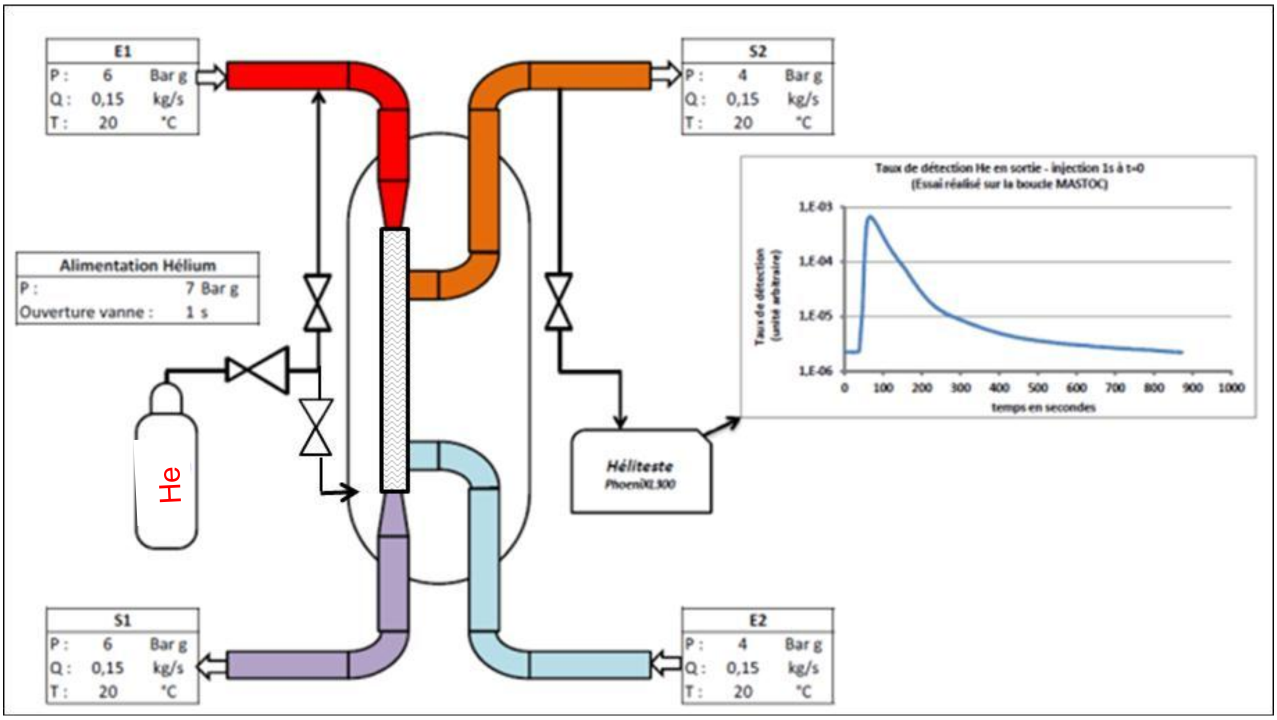

Figure 34 : Recall of the leak detection

A specific procedure was applied to periodically check the state of the HX by injecting, each time, the same amount of helium and looking to see if the outlet signal evolves or not.
During manufacturing of the HX, a very small leak was detected by Alfa Laval. This leak has no effect in term of the global performance of the HX and it was decided with the partners' agreement not to repair it since it could have been more damaging. This default is in fact an opportunity for us to calibrate the helium leak detection. It enabled us to calibrate the system (amount of helium and duration of helium injection). Since we have a plot of the response time, this is used as a reference. The superposition of the different measurements allowed us to check if there is an evolution or not of the leak. The method is considered as a qualitative and not quantitative solution as we cannot estimate the size of a leak.

The leak detection has to be carried out when the loop has cooled down so it requires time and therefore cannot be repeated very often to avoid loss of time. At the end of a specific campaign, the loop was cooled down over the whole week end and the leak detection test was made on Monday and the next steady thermal test was reached on the following Tuesday or Wednesday. Hence the leak detection test was made as follows:

- Before beginning of the first increase of temperature → reference point
- At the end of the transient shocks run at T hot =650°C
- At the end of the transient shocks run at T hot =700°C
- At the end of the transient shocks run at T hot =750°C
- At the end of the transient shocks run at T hot =800°C

When helium is injected into one circuit, the operation is repeated 10 times to check the results.

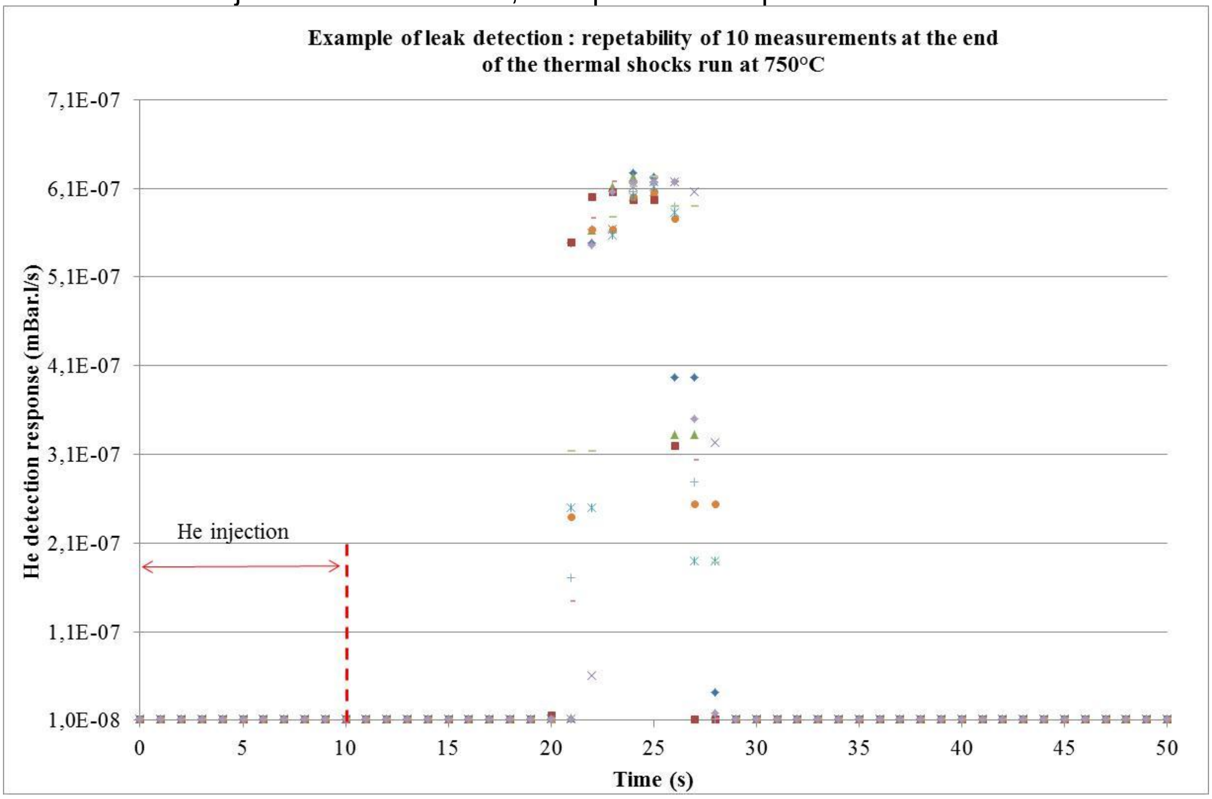

Figure 35 : Example of 10 successive measurements showing the good repeatability of the test

Figure 35 shows the evolution of the signal delivered by the leak detector device. It should be remembered that there was a small leak which was detected during manufacturing of the mock up corresponding to the “reference signal” on the next figure. The leak was detected within the bundle between hot and cold circuits and our device allows tracking of the evolution of this leak (or maybe the start of another one…).

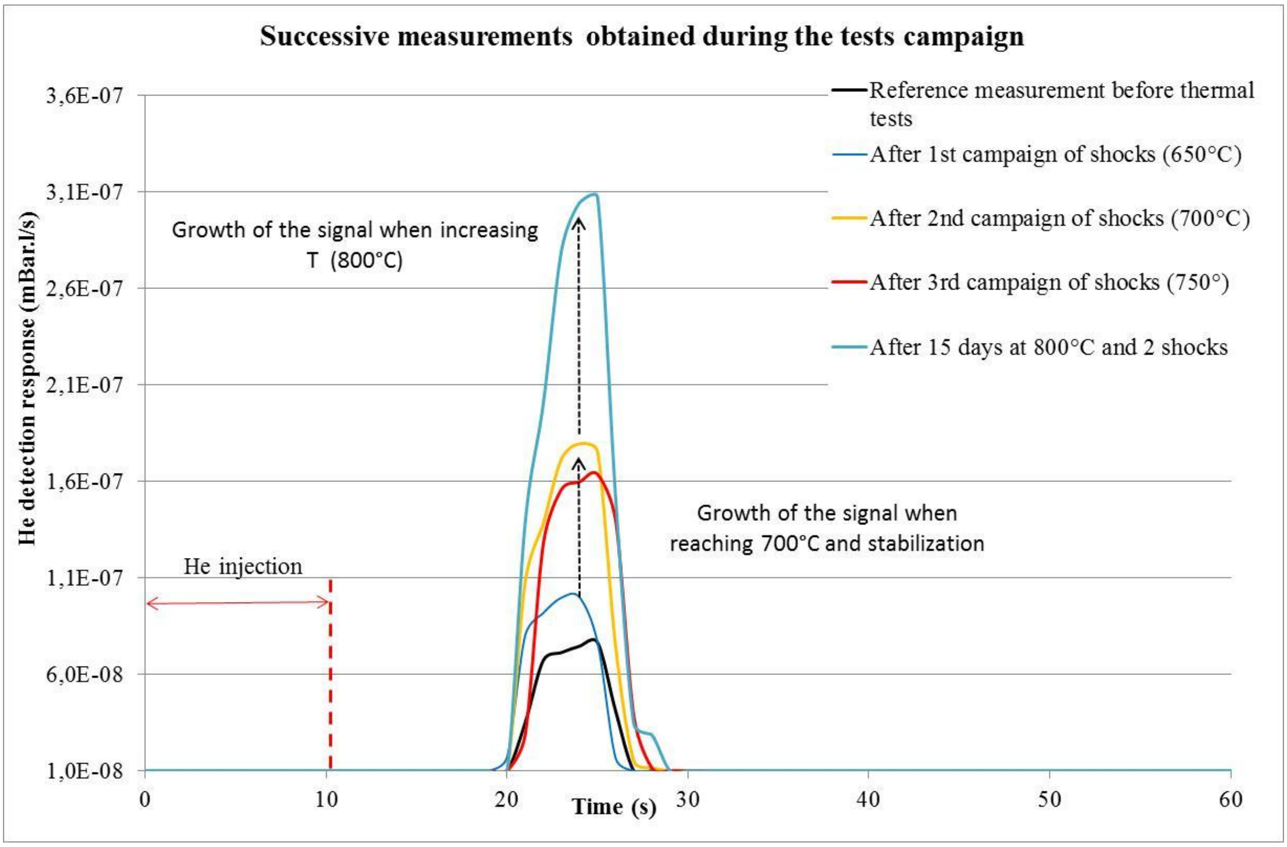

Figure 36 : Evolution of the leak detection response with time

Figure 36 shows that the signal area has increased progressively when running the transient tests and more especially during first and second transient campaigns. Between the two last series of tests, the signal seems to be stabilized.

After running steady state tests at 800°C and 2 shocks, we see a second important increase of the signal. The detection of the leak always occurs at the same time and the width of the signal is still the same. This initial leak is located in the cold part of the heat exchanger.

The leak is growing but we may think that no other fissure has appeared and more especially in the hot part of the heat exchanger.

The leak is detected within the bundle whereas nothing is detected from the shell to the secondary circuit through the wall.

8. CONCLUSION

Thanks to the EC ARCHER project, a significant size compact heat exchanger was manufactured by Alfa Laval and was tested by CEA in the air Claire test facility located at Grenoble. Preliminary numerical simulations were carried out to estimate the thermal and mechanical behavior of such a component. Initial tests were dedicated to determine friction and thermal performance of this stamped plate heat exchanger. The measurements obtained during these tests are expressed under dimension less numbers so that the extracted laws are independent of the fluids and of the working conditions (i.e. temperature and pressure). With regard to thermal and friction performance obtained from the CFD calculations (not in the frame of ARCHER), we obtained a good agreement between measurements and calculations.

From the thermal point of view, the heat exchanger provides the expected thermal efficiency of 90% in the whole range of Reynolds number. The prototype was sized in relation to a real He He IHX, in terms of its plate dimensions and range of Reynolds number.

From thermo mechanical point of view, it was decided, in agreement with partners of the project, to progressively increase the working conditions to avoid early damage. Therefore, both the level of temperature and the amplitude of temperature variations during thermal shocks were increased progressively.

The heat exchanger was submitted to a large numbers of shocks (around 170 with various thermal conditions). Using helium leak detection, it was possible to have an idea of the damage caused by the shocks. During manufacturing of the prototype, a very small leak was detected by Alfa Laval in the cold part and to avoid further damage it was decided to not repair it. This small leak between primary and secondary sides was used as a reference signal during tests campaign to judge whether an additional leak had occurred. The signal increased with time indicating a growth of the initial leak but apparently no other ones occurred and more especially in the hot part.

Looking at the measured temperatures on the external end plate of the bundle, an important thermal gradient compared to the CFD calculations was identified. The temperatures are strongly affected by the boundary conditions inside the bundle, and the internal and external insulation were not efficient enough to limit these effects. Therefore, it is considered much more difficult to validate experimentally the FEM calculations.

The Alloy 800H compact stamped plates mockup has been a technological challenge both to manufacture and to test to show its ability to withstand such working conditions at higher temperatures and gradients than those predicted for the IHX during operation. Nevertheless, this has been successfully achieved and it is considered that further analysis and investigation will be needed before the integrity and lifetime of the mockup and full size IHX can be fully evaluated.

At this time, thermal tests on the prototype are still going on.